

# Report of simulation investigations, part II, a growth of half-chaotic autonomous networks

Andrzej Gecow

<https://sites.google.com/site/andrzejgecow/home> [gecow@op.pl](mailto:gecow@op.pl) [andrzejgecow@gmail.com](mailto:andrzejgecow@gmail.com)

This is the second part (<http://vixra.org/abs/1711.0467>) of the **report** which is planned to grow. This is **chapter 8** of this whole, it is a documentation of the ‘method 8’ - ‘**met8**’ of research carried out in 2015-2017. First part - **rep** (<http://vixra.org/abs/1603.0220>) describes the ‘**met1-7**’ study done by the author in 2011-2015, which is the basis for article **Naaj** (<http://vixra.org/abs/1612.0390>).

If next parts will appear, then here I will add links to them. Next one – ‘**met9**’ should be about structural tendencies in growth of open half-chaotic networks. This part II, **rep** and **Naaj** have also version in Polish.

Reading this report without reading short article **Naaj** and briefly look on large **rep** would be a rather ineffective effort. This material simultaneously fulfills two tasks: it is a publication that can be quoted referring to the materials posted here; and above all, this is complementary material to ordinary publications like **Naaj** which are only planned. The specific form dedicated to reading on a computer screen is tailored to the second task, so that specific problems or uncertainties can be analyzed as accurately as possible. The drawings should be analyzed in enlarged form. The study of modularity in the ‘met8’ (ch.8.5) leads to correction of part I (to v5-Pl and v6-Eng) - replacement of firstly used name ‘**semimodularity**’ by more adequate ‘ro-modularity’.

## Abstract

In the first part: “Report of simulation investigations, a base of statement that life evolves in half-chaos” networks have constant structure. Deviations from their randomness are found in correlations of states and functions of nodes, the change initiating the damage consists of a small change in the node function. Here we also come from the point attractor, but the initiation change is a random addition or removing the node. The networks grow and in them also half-chaos occurs, which is an important complement to the arguments found in the part I. Now structure is changed and the evolution with the condition of a small change keeping the half-chaos creates structural tendencies such as the greater conservativeness of the older nodes. The classic modularity, its source and its connection to ro-modularity are also found.

**Keywords:** chaos; complex networks; dynamic networks; deterministic networks; Kauffman networks; computer simulation, growing networks, structural tendencies, modularity.

## Contents

For the continuity of the report it contains the titles of the main chapters of part I, and the actual content of this part. II is chapter 8, however, References and Some strange names or shorts and typical parameters are mainly for part II. I believe that the "Table of Contents" significantly facilitates the idea of the whole and navigation.

Abstract .....	1
Contents.....	2
The main chapters in the part I of Report.....	3
<b>1 Introduction .....</b>	<b>3</b>
<b>2 Negative feedback density increasing - met1 &amp; 2 .....</b>	<b>3</b>
<b>3 Modularity – met3 .....</b>	<b>3</b>
<b>4 Point attractor – met4 .....</b>	<b>3</b>
<b>5 Accumulation of ordered changes does not lead to chaos, ro-modularity – met5.....</b>	<b>3</b>
<b>6 Start from the short attractor instead PAS0 – met6.....</b>	<b>3</b>
<b>7 Controlled creation of ro-modules – met7 .....</b>	<b>3</b>
References .....	4
Some strange names or shorts and typical parameters .....	5
<b>8 Initiation through addition and removing of nodes – met8 .....</b>	<b>6</b>
8.1 Aims .....	6
8.2 Algorithm .....	6
8.2.1 Basic assumptions of the algorithm.....	6
8.2.2 Problem of removal for sf.....	7
8.2.3 Problem of oscillating processes near the threshold .....	7
8.3 Results in half-chaos aspect .....	8
8.3.1 Distributions P(d), q, P(k) and ice .....	8
8.3.2 Fade out and secondary initiations.....	13
8.3.3 Observations of crocodiles .....	16
8.4 Tendencies .....	22
8.4.1 Tendency of conservativeness of older nodes.....	22
8.4.2 Comparison of modularity effects .....	24
8.5 Modularity studies ‘met58ro’ for models c and b .....	36
8.5.1 Sources of modules presence in random networks and their relationship to 'ro-modules' .....	36
8.5.2 Simulation results for ss and lv networks complementing met5 results .....	39
8.6 Summary .....	41

## **The main chapters in the part I of Report**

They describe the consecutive "methods" in accordance with the development of research, but I often returned to previous methods, supplementing them with new tools mastered in the later stages. In part I, the network structure remained constant and the initiation consisted of a small permanent change in the function of the node.

### **1 Introduction**

Includes: Substantive introduction, where I point to the initial theses and motives of undertaking this research. This is mainly the conflict of assumptions of my earlier studies of structural tendencies with the well-known and shared Kauffman hypothesis: "life on the edge of chaos and order." Who is right - me or Kauffman. These tests give right for me. Organizational introduction, where I describe the form of the report and its assumptions.

### **2 Negative feedback density increasing - met1 & 2**

An attempt to check the original thesis (that stability is mainly due to regulation in systems even with parameters that give chaos, rather than "order" without this regulation) by converting the feedback into negative. This thesis proved to be insufficient, and the diagnosis indicated the role of the short attractor.

### **3 Modularity – met3**

The short attractor could have resulted from small modules, i.e. from modularity, but it turned out (provisionally) to be usually insufficient, even assisted by met2.

### **4 Point attractor – met4**

Initially, it was a new attempt to introduce negative feedbacks differently, but it turned out that the point attractor alone was enough.

### **5 Accumulation of ordered changes does not lead to chaos, ro-modularity – met5**

The study of evolution coming out of the point attractor - the accumulation of initiating changes that give small damage. This study defined half-chaos and confirmed the importance of the small attractor, indicated the mechanism of ro-modularity.

### **6 Start from the short attractor instead PAS0 – met6**

Checking if starting from the short attractor is enough to get half-chaos. It turns out that it is enough, but such half-chaos is indeed less useful for modeling.

### **7 Controlled creation of ro-modules – met7**

Effective attempt to build ro-modularity and half-chaos on the basis of the ro-modularity mechanism recognized in met5.

## References

- Barabasi-Albert** A.-L. Barabási, R. Albert, H. Jeong, 1999. Mean-field theory for scale-free random networks. *Physica A* 272, p.173–187.
- Derrida** B. Derrida, Y. Pomeau, 1986. Random Networks of Automata: A Simple Annealed Approximation. *Europhys. Lett.*, 1(2), p.45–49.  
B. Derrida, G. Weisbuch, 1986. Evolution of Overlaps Between Configurations in Random Boolean Networks. *Journal De Physique* 47, p.1297–1303.
- Erdos-Renyi** P. Erdős, A. Rényi, 1960. Random graphs. Publication of the Mathematical Institute of the Hungarian Academy of Science, 5, p.17–61
- Hughes00** T. R. Hughes et al., 2000. Functional discovery via a compendium of expression profiles. *Cell* **102**, p.109-126.
- Kauffman 1969** S.A. Kauffman, 1969. Metabolic stability and epigenesis in randomly constructed genetic nets. *J. Theor. Biol.* 22, p.437-467
- Kauffman 1971** S.A. Kauffman, 1971. Gene regulation networks: a theory for their global structure and behaviour. *Current topics in dev. biol.* 6, p.145.
- ooKauf** S.A. Kauffman, 1993. *The Origins of Order: Self-Organization and Selection in Evolution.* (Oxford University Press New York)
- Ramo06** P. Rämö, J. Kesseli, O. Yli-Harja, 2006. Perturbation avalanches and criticality in gene regulatory networks. *J. Theor. Biol.* **242** p.164-170
- Serra04** R. Serra, M. Villani, A. Semeria, 2004. Genetic network models and statistical properties of gene expression data in knock-out experiments. *J. Theor. Biol.* 227, p.149-157
- Serrajtb07** R. Serra, M. Villani, A. Graudenzi, S. A. Kauffman, 2007. Why a simple model of genetic regulatory networks describes the distribution of avalanches in gene expression data. *J.Theor.Biol.* **246** 449-460
- arj** A. Gecow, 2010. More Than Two Equally Probable Variants of Signal in Kauffman Networks as an Important Overlooked Case, Negative Feedbacks Allow Life in the Chaos. [arXiv:1003.1988v2](https://arxiv.org/abs/1003.1988v2)
- brj** A. Gecow, 2010. Complexity Threshold for Functioning Directed Networks in Damage Size Distribution. [arXiv:1004.3795v1](https://arxiv.org/abs/1004.3795v1)
- it** A. Gecow, 2011. Emergence of Matured Chaos During Network Growth, Place for Adaptive Evolution and More of Equally Probable Signal Variants as an Alternative to Bias p. In: *Chaotic Systems*, E.Tlelo-Cuautle (ed.), ISBN: 978-953-307-564-8, pp 280-310.
- 1975** A. Gecow, 1975. A cybernetic model of improving and its application to the evolution and ontogenesis description. In: *Fifth International Congress of Biomathematics Paris.*
- krab** A. Gecow, M. Nowostawski, M. Purvis, 2005. Structural tendencies in complex systems development and their implication for software systems. *Journal of Universal Computer Science*, **11** p.327-356.
- dgec** A. Gecow, 2008. Structural Tendencies - effects of adaptive evolution of complex (chaotic) systems. *Int.J Mod.Phys.C*, 19, 4, pp 647-664.
- bics** A. Gecow, 2008. A simplified algorithm for statistical investigation of damage spreading. *BICS 5-7 Nov.08 Tg.Mures Romania AIP Conf. Proc.* 1117 pp 133-141.
- fgec** A. Gecow, 2009. Emergence of Chaos and Complexity During System Growth, pp 115-154. &
- ggec** A. Gecow, 2009. Emergence of Growth and Structural Tendencies During Adaptive Evolution of System, pp 211-241  
In : *From System Complexity to Emergent Properties.* M.A. Aziz-Alaoui & Cyrille Bertelle (eds), Springer, Understanding Complex Systems Series
- rep** A. Gecow, 2016. Report of simulation investigations, a base of statement that life evolves, in half-chaos. <http://vixra.org/abs/1603.0220>.
- Naaj** A. Gecow, 2016. Life evolves in half-chaos of not fully random systems. <http://vixra.org/abs/1612.0390>.
- GdM** M. Nowostawski, A. Gecow, 2011. Identity criterion for living objects based on the entanglement measure. *ICCCI 2011, Studies in Computational Intelligence* 381, Radosław Katarzyniak, Tzu-Fu Chiu, Chao-Fu Hong, Ngoc Thanh Nguyen (Eds.) *Semantic Methods for Knowledge Management and Communication*, Springer, pp 159-170.

## Some strange names or shorts and typical parameters

**s** – number of signal variants. They should have the same probability. **K** – number of input links in each node of network. **s,K** – two dimensional parameter (s,K).  
**k** – number of node outputs, for network ak, al and lv k=K.

**N** – number of nodes in network. **tmx** – number of observer time steps, maximal time, length of investigated section of trajectory.

**net types:** **sf** – scale free, [Barabasi-Albert](#), **ss** – single scale, **er** – “Random” [Erdos-Renyi](#) (not used in the main met8, only in met58), **ak** – „aggregate of automata” in Kauffman form (k=K). **sf**, **ss**, **ak** with node removing are marked accordingly **sh**, **si**, **al** (ch.8.2.1). In met58 (ch.8.5.1) special form **lv** of **ak** is used.

In the figures, the types are marked with one, the second letter only.

**reversed-annealed algorithm** see [\[arj ch.3\]](#) [\[dgec, bics, fgec, it\]](#)

**ini** – initiation, in met8 it is addition or removing of node; in met1-7 permanent change of function value for one node, for one input state.

**PAS** – Point Attractor System, network where each current node state is equal the node function value for current input state. Attractor length =1. See ch.4 of [rep](#).

**PAS0** – PAS where each current node state = 0 (and each current node input state contain all K input signals=0), not used in main met8.

**d** – **damage** – fraction of nodes which node state differs between observed disturbed network and pattern – original, not disturbed network.  $d=A/N$ ,

**A1** – **Avalanche** – number of damaged node (state of the node differ to pattern) in particular t. **A3** – A1 averaged on the last 50 time steps.

**Threshold** – arbitrarily taken number (from the gap between **left** and **right peak** in damage size distribution) which differs small (ordered) and large (chaotic) effective change in  $A(tmx)$ . In met8 threshold=0.2 and 0.5 of actual N.

**Accepted ini (akc)** - which has  $A(tmx) < \text{threshold}$ .

**q** = (number of accepted ini)/(all ini). Stability is measured using **order degree q** (symbol used as in [\[Ramo06 see ch.2\]](#)).

**met8** – Method 8 of half-chaos search. From met2 to met8 they are described in chapter 2 to ch.8 respectively.

**explosion** – rapid come of process  $A(t)$  from small difference to pattern (order) to large difference (chaos).

**crocodile** – useful form  $A1(t)$  of image of simulation, see ch.8.3.3, wider description in ch.4.4 of [rep](#).

**half-chaos, ro-modularity** – see ch.1.1 of [rep](#), here ch.8.5, and other introductions.

References to the figures are marked in red, in the range of met8 (of this, part II of the report) they are numbered from 1, references to earlier chapters in Part I precede m with the number of the chapter, e.g. **m3.fig.2** refers to fig.2 in chapter 3 (met3).

In most of figures colon separating integer form decimal parts is replaced by comma, due to polish version of Excel, sorry.

## 8 Initiation through addition and removing of nodes – met8

### 8.1 Aims

The met1-7 study was caused by the weak basis of the reversed-annealed algorithm I used earlier (1974-2009) for research mainly on the adaptive evolution of the open system evaluated at the outputs. At that time, there was no other way to be seen and a strong simplification was necessary. Also to the defense of the PhD thesis whose results were published in the following years, the widely accepted Kauffman hypothesis that life is on the edge of chaos and order was not known at the moment. However, the rev-ann algorithm build on the basis of heuristic premises practically assumed the presence of both mature chaos and, at the same time, order in the same system. Such a possibility is excluded in the image of a random Kauffman network, where there is a phase transition between order and chaos, and the system can only be either orderly or chaotic. However, living objects should not be treated as completely random due to natural selection. The basic aim of the search for the 'met' series was to show that there are systems that are not fully random, which at the same time present mature order and chaos in a similar degree. The task was limited to autonomous systems, because the controversial Kauffman hypothesis concerns such systems.

It has been shown [rep,Naaj] that within autonomous systems with a random permanent structure, one can create half-chaotic systems for changes initiated by a permanent point change of functions by selecting functions and states of nodes, respectively. The half-chaotic system has the parameters of a random chaotic system, but a significant part of the initiation behaves as in an ordered system. In research on structural tendencies, the questioned rev-ann algorithm was used to increase the system, where the initiating changes were the random addition of nodes, as well as the removing of nodes. A natural complement to the met1-7 study is to check that half-chaos also occurs in such initiations (still in the field of autonomous systems), which is the task of **met8**. At **met9**, the study of open systems is planned.

**Up to now (met1-7) the structure was constant**, the research concerned the correlation of nodes' states and functions. This permanent structure was random, only the modularity study in met3 formed a non-uniform structure. **Currently**, using the addition of nodes, we enter the study of network growth, so the structure ceases to be constant, where attachment (or disconnection) is covered by the condition, which causes **the resulting structure to cease to be random**.

### 8.2 Algorithm

#### 8.2.1 Basic assumptions of the algorithm

In the met8 study we start from the point attractor system (PAS), similarly to met5, but it can not be PAS0, since removals would then always be allowed. At the initial stage, a network of 50 nodes is built according to the rule of a given type. Then, the initial states and functions are drawn – we get fully random network. Now the functions for the initial state of the input of each nodes are changed to give their initial state (i.e. the states of nodes from the moment  $t = 0$  and  $t = 1$  are to be the same). This creates a PAS. The addition of nodes for sf, ss and ak is further drawn, and for sh, si, al which are respectively sf, ss and ak for addition, also removal of nodes, whose share is 30% (for al only 10%). The rules for adding and subtracting nodes are described mainly in [it.fig.2], earlier in [brj.fig.1, ggec.fig.4]. The networks of s,K = 4,3 are tested, only for ak and al, also 4,2. As from met5, the shift by  $t = 50$  of trajectory beginning after accumulation is used.

To achieve at least length 7 the attractor can not decrease, it still can not fall below 7, but when this condition blocks the accumulation too long (more than 60 times), the currently proposed attractor less than 7 is allowed and again it can not decrease until it not exceeds 7.

Further growth of network is divided into 10 passes, in which the network increases by next 50 nodes, so that it ends on the value  $N = 550$  nodes. These are passes 2-11 indicated on crocodiles and tracked dynamically, but to analyze the collected data it turned out that they are too small (apart from the modularity test in chapter 8.4.2). In such an analysis presented further, the graphs use the stages M1-5 created by summing up two successive passes of the tracked evolution, so that M1 is pass 2 + pass 3.

During the preliminary, reconnaissance simulations, the threshold was set at 0.4 of current  $N$ , however, the problem of filling the interval between left and right peaks in the damage distribution discussed in Fig.2 led to selection in the main simulation of the threshold  $0.2N$  and comparison of results for the threshold  $0.5N$ . Crocodiles in Fig.6a-c are still with a threshold of 0.4, in Fig.6d-e - with a threshold of 0.2, and in Fig.6f - with a threshold of 0.5. The scale on the left in these figures applies to the maximum  $N$  in the given pass. In addition, the distribution of nodes degrees  $\#k$  for 11 smallest  $k$  (0-10) is dynamically shown, and over the crocodile the range of  $N$  - the last 50 nodes, which illustrates the increase, below - ice on the scale  $N = 50$  pixels, and even lower on the scale 50 pixels down  $k = 0, 1, 2$  and 3. Ice and degree  $k$  are only shown for acceptable. These views were to facilitate the identification of correlations and mechanisms. Details of modification of the algorithm for modularity tests are described in Ch.8.4.4.

## 8.2.2 Problem of removal for sf.

The er network, which until now was the only one with blind nodes (nodes without outputs, with  $k = 0$ ), can not be used in met8 because it does not have the rule of growth (adding new nodes to the already existing network). In sf, ss and ak networks, the addition of new node is the rule for the creation of a network that determines their type and distribution  $P(k)$ . The ak network has a fixed  $k$  and simple removal rule that does not change the uniform  $k$  value for all network nodes. The problem arises when we demand the removal of nodes in sf and ss networks, which creates networks sh and si. As a result of node removals nodes with  $k = 0$  arise. In the case of a network where the addition rule (ss) links a new node with other nodes present in the network with equal probability, blind node can recover the output, but in the network sh (connection proportional to  $k$ ) no longer has the chance for output and can only be removed like every blind nodes. In order to make the rule for sh more real, an addition was done in proportion to  $(k + 1)$ . In all three cases, each node has the same probability of removal, which for sh and si may change the shape of  $k$  distributions, it causes that they lose the original properties associated with the types sf and ss. This verifies Fig.3.

## 8.2.3 Problem of oscillating processes near the threshold

In the studies from met1 to met7, the process that crossed the threshold almost never came back under him. This allowed for the optimization and interruption of counting of those that were above the threshold after 70 steps from the first cross. At that time, they could go down and stay there, but it never happened, and the size of the fluctuation was usually so small that it did not reach the threshold. This was due to the size of the resulting ro-modules. Only in met3, where modules were constructed (created arbitrarily) the image was different (m3.Fig.2 and 3), there were often lower levels of Derrida equilibrium around the threshold, but there was no deeper investigation of this model. In the met8 study, however, there are relatively frequent cases of larger ro-modules (or modules, see Fig.6c-f, ch.8.4.2), where the fluctuation range after crossing the threshold is so large that the threshold level is often crossed and the chance of the fact that in tmx A1 (the temporary value A - the number of nodes with the state different from the pattern) will be just below the threshold, it is considerable. Such cases should be eliminated by the criterion A3, which is the average of A1 on the last stretch of 50 counting steps. It turns out, despite the A3 below the threshold, that the frequent presence of the process above the threshold allows to create a pattern after accumulation and shift, which with a much higher probability also leads to large ro-modules, and even chaotic collapse (Fig.6e5, f1-4). These large 'ro-modules' strongly suggest that maybe they are also classic modules that have the right to arise under the influence of evolutionary pressure resulting from the condition of small change. Such a hypothesis is examined in chapter 8.4.2 and partially turns out to be correct.

For the purity and simplicity of acceptance and accumulation criteria, a rule has been introduced that the process that has returned under the threshold is still counted, and its counting ceases after 70 steps since the last transition over the threshold. This caused that a large part of such processes, even with A3 over the threshold, was counted for a long time, even to the end (Fig.6c1, d1).

The presence of processes oscillating around the threshold causes "backfilling" gap in the distribution  $P(A3)$  (the form of the distribution  $P(d)$  – of damage size, Fig.1b, 2). The gap between the left and right peaks has significant interpretive meaning in the half-chaos concept. It allows for the natural criterion of elimination and maintenance of half-chaos - the evolutionary stability of half-chaos observed in met5-7. Backfilling this gap caused that the threshold position became meaningful and ceased to be well-defined and the responsibility fell on its arbitrary choice. Instead of, therefore, the  $0.4N$  threshold used in the initial simulations, the thresholds  $0.2N$  and  $0.5N$  (Fig.2) were used to compare the effect of this arbitrary choice. As you can see, the low threshold allows for smaller backfilling of gap between the peaks, but it is clearly arbitrary, even on the fall of the left peak. Moving the threshold according to this diagnosis close to the minimum gives a different picture, in which additional peaks are created in this area in the sh and si networks. They are small compared to the right and left peaks, but several times greater than for the smaller threshold. The minimum separates into two complicating interpretations, and for met8 the evolutionary stability of half-chaos and the criterion of identity are slightly weaker. You can blame the size of the initiating change, which is the addition or removal of the node, so it is not a small change, and it can not be reduced. The threshold of  $0.5N$  was used to study the effects of modularity in Ch.8.4.2, because it gave a wider range for testing, not intensely colliding with the threshold.

### 8.3 Results in half-chaos aspect

This chapter describes the results of the occurrence of half-chaos with its evolutionary stability also in the case of initiations consisting in the addition and removal of nodes, more generally - on structure changes. This is an important supplement to the met4-7 studies introducing half-chaos, especially since these are not very small changes.

#### 8.3.1 Distributions $P(d)$ , $q$ , $P(k)$ and ice

The basic simulation series contains 600 networks of type sh, si, al2, al3, sf, ss, ak2, ak3. Except al2 and ak2 where  $s, K = 4,2$  ( $K$  indicates an additional digit) in the remaining cases  $s, K = 4,3$ .

It is assumed as stages M1 - M5 a 2 passes of 2-11 from crocodiles increasing  $N$  by 50, so that  $M1 = \text{pass2} + \text{pass3}$ , network grow by 100 nodes.

**The basic results are:**

**$P(A3|\text{type})$  distribution** (i.e. practically and more adequately:  **$P(d|\text{type})$** , Fig.1ab and 2c) for the stabilized stages M2 to M5, further analyzed in more detail in Fig.2ab in the form  **$P(A3|M)$**  for particular type and threshold  $0.2N$  and  $0.5N$ ; compared with the result  **$P(A3|\text{type})$** . This is the **damage size distribution** measured by the value  $A3$  for comparison and uniformity with the results of previous methods, however here  $N$  grows and  $A3$  is normalized to  $N = 200$ , which simply corresponds to ' $A3$ ' =  $d * 200$ . In Fig.1a, the scale  $d$  was added, but the remaining figures were left so normalized  $A3$ . The initial stage M1 turns out, as usually, slightly different, which can be clearly seen in Fig.2, 3ab and Fig.4a-e, further stages are already similar and can be combined. The image of the left peak is similar for all stages even on the log scale (Fig.2ab).

**$q(\text{type})$**  Fig.1d is calculated from the above  $P(A3|\text{type})$  based on the threshold in  $A3$  assumed as 0.2 of the current  $N$ , i.e.  $d = 0.2$ . For the sh and si network, it contains a piece resulting from  $k = 0$ . **This is the basic result showing a significant presence of order, which mainly distinguishes half-chaos from chaos.**

**$q(M)$**  Fig.2d, 4a shows the obtained degree of stabilization of evolution (see for comparison m5.Fig.4a, m6.Fig.1a, m7.Fig.9h), **allows to state that the evolution was carried out long enough.**

**$q(t)$**  Fig.4h and crocodiles Fig.6 show the obtained degree of stabilization of the process after the disturbance and **are the basis for recognizing tmx as sufficient**. This problem was also examined, as in met5-7 (m5.Fig.5a, m6.Fig.1c, m7.Fig.17d), through the range of  $t$  of explosion to chaos - the average  $t$  for the five latest explosions (Fig.2f, 4b). Here, similarly - in the M2-5 range, this average time practically does not grow.

**ice distribution:  $P(\text{ice size}|\text{type})$**  Fig.4fg,  **$\langle \text{ice} \rangle (M|\text{type})$** , Fig.2e, 4c, 9h3. **This is the main argument for the similarity of the mechanism studied in met5 and 7, called the ro-modularity.** Only for the ss network, the average ice in the studied range of evolution is clearly declining, which may raise anxiety about whether this decrease will stop at the level that still entitles to the mechanism of ro-modularity and evolutionary stability of the so-obtained half-chaos, it should be noted that the scale in Fig.2e, 4c begins above the middle of the range.

**$P(k|\text{type})$**  Fig.1c, analyzed more precisely as  **$P(k|M)$**  in Fig.3, first of all justifies the use of the names of the types sf and ss and indicates the deviations from sf and ss which the removal of nodes in the types sh and si introduces.

**More detailed analysis in descriptions of figures.**

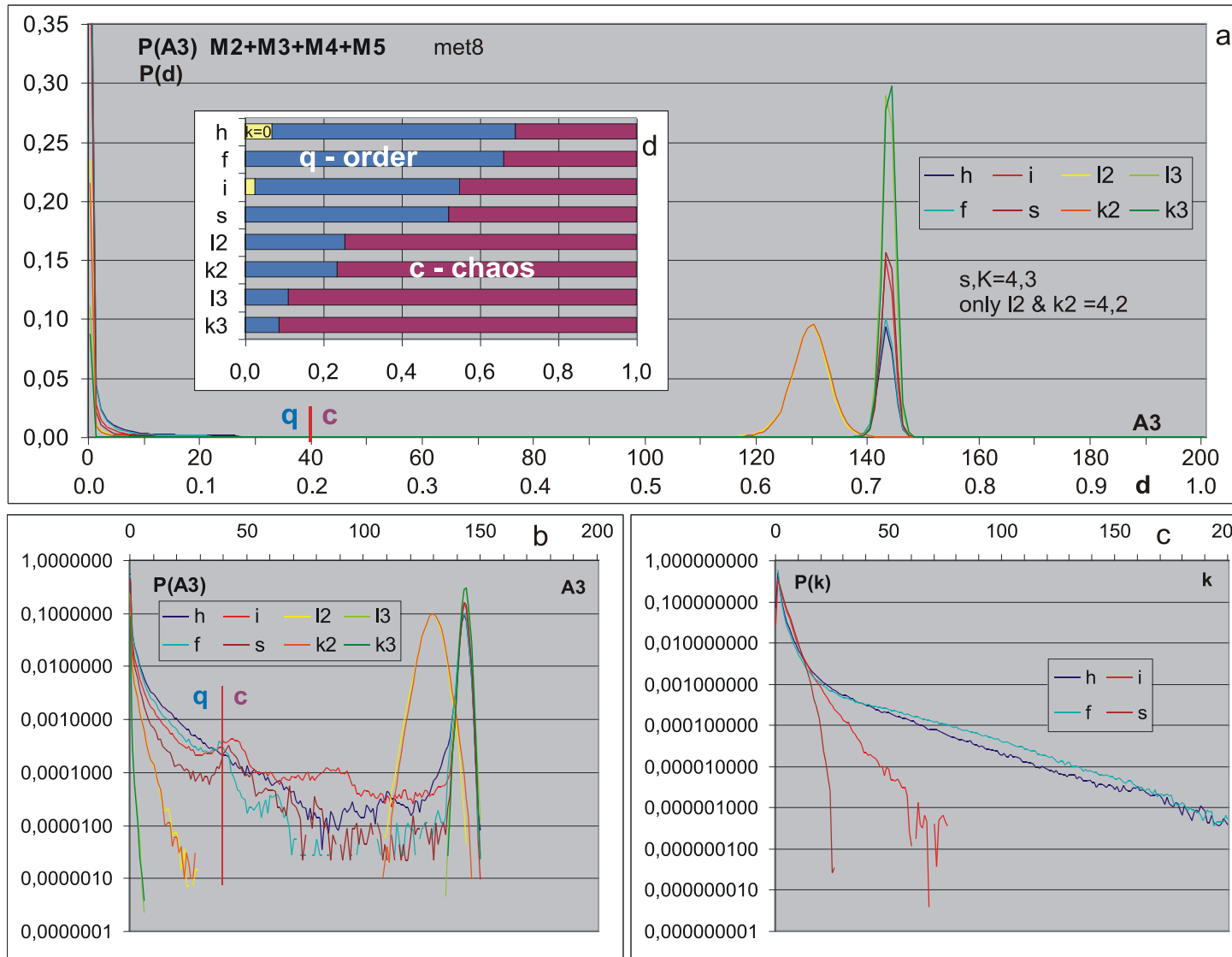
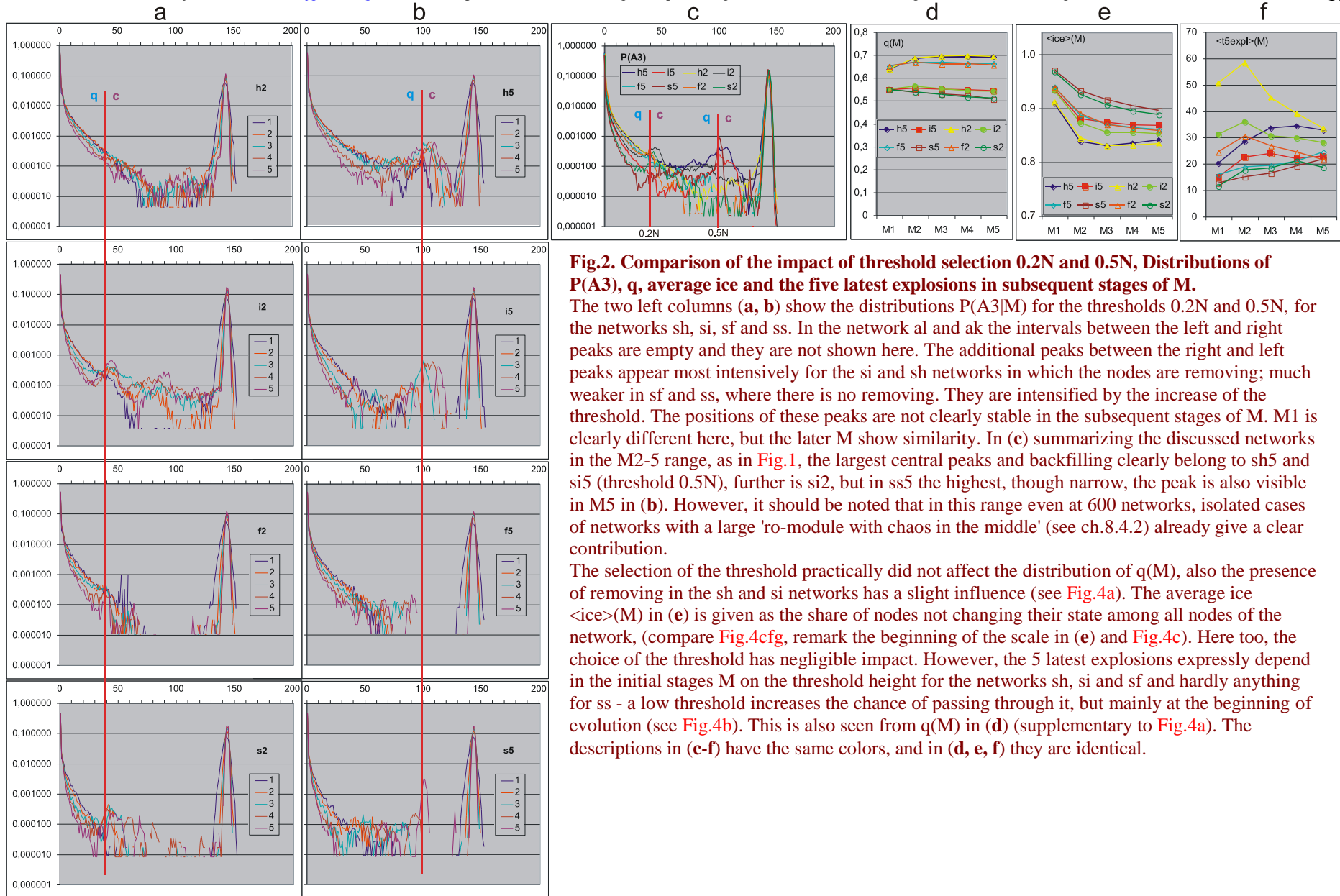


**Fig.1. Damage size distribution P(d) in the form P(A3).** Generally in met8  $s, K = 4,3$ , but the networks al & ak are also present in  $s, K = 4,2$ , which distinguishes the digit corresponding to K. As previously, I use only the second letter of the network type abbreviation. The M stages are the sum of the two passes visible in Fig.6 -crocodiles. E.g. M1 is pass 2 - increases from  $N = 50$  to 100 and pass 3 further increases to 150. M1 gave slightly different results from later M (see Fig.4a-e), so like in met5-7 it was omitted in the summary, which includes an increase from  $N = 150$  to 550. The networks sh, si, al (h, i, l) have the removing of nodes, sh and si 30% of the proposed changes, and al 10%, they correspond to the networks sf, ss, ak without removing.

(a) - Similarly to m5.Fig.20 and m7.Fig.1, 9, it presents a full distribution of P(d) in the version P(A3) in a linear scale with pasted (d) share of q-order and c-chaos. Because the network here growing, the horizontal axis scale is also shown in more adequate d (range 0-1). The value A3 was imported in each process ( $A3/N*200$ ) to the range of 200, i.e.  $A3=d*200$ . The threshold 0.2N (i.e.,  $d = 0.2$ ) in this scale falls on the values of  $A3= 40$ .

(b) - presents the same as (a) in the log scale for the assessment of the gap depth between peaks, the location of the threshold and the shape of the left peak. In the vicinity of the threshold you can see additional peaks, which are more closely analyzed in Fig.2, where the results for the threshold 0.5N are also shown.

(c) - Distribution of degrees k of nodes, i.e. the number of outputs from the node, in the log scale. This is more accurately analyzed in Fig.3. In the case of network sh and si  $P(k=0)$  is 0.08 and 0.034 respectively, which is marked in (d) in yellow as the order of other origin. As you can see, the share of order q is significant and larger in networks with removing. For the network of al and ak, especially with the larger K is already very small, but significantly larger than in the chaos, where on such a show it would not be visible at all (see m7.Fig.1).



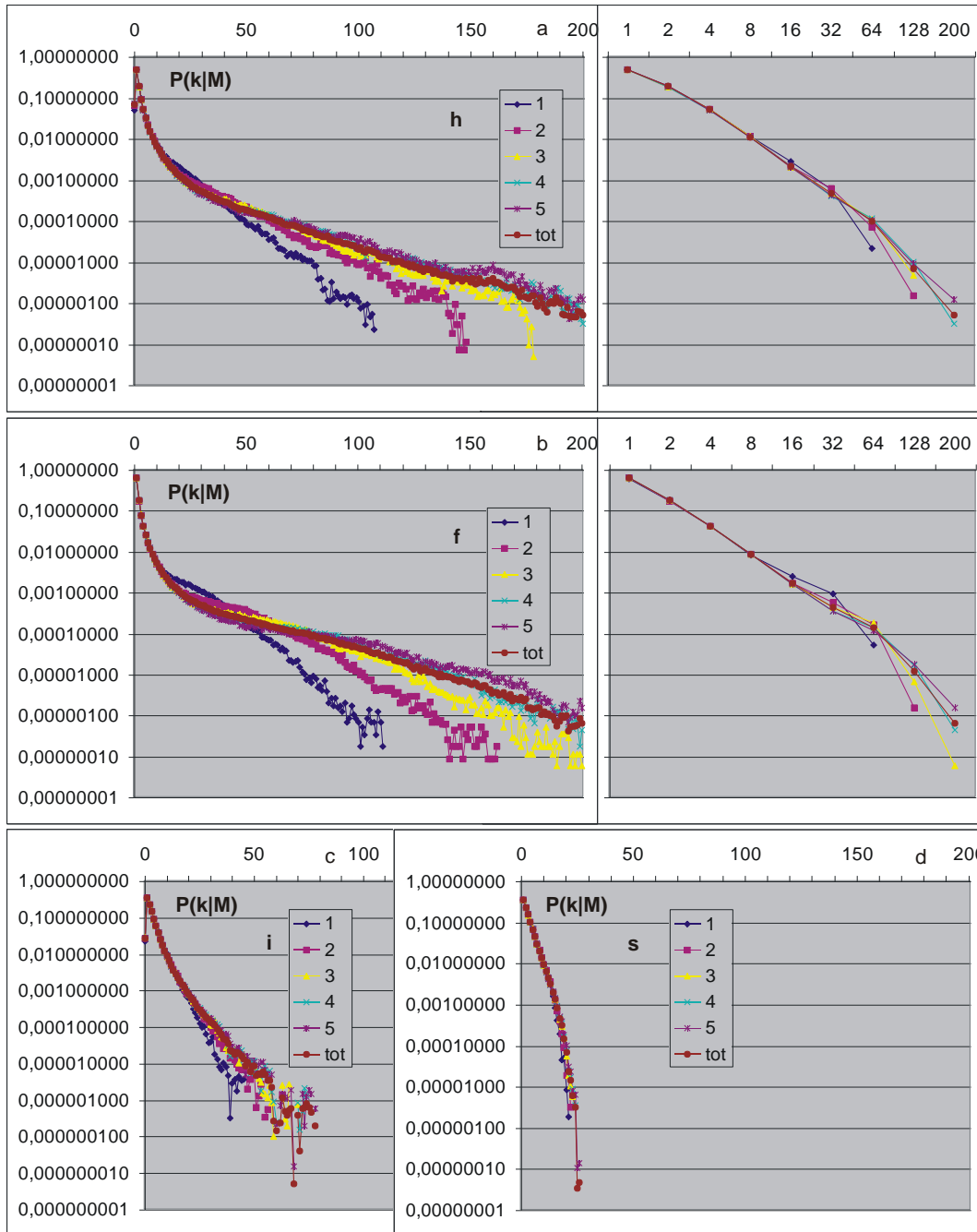


**Fig.3. Distributions of node degrees depending on the stage M -  $P(k|M)$** , presented mainly in order to indicate to what extent the process of evolution (accumulation) reaches a stable state in this aspect. The second task is to justify the use of the names sf and ss, which in addition to the rule of growth are characterized by just the appropriate distribution  $P(k)$  (compare with Fig.1c).

Clearly the M1 stage is sticking out, M2 is also a bit out of place, but these deviations appear for larger  $k$  which have very small probabilities and therefore a small share. These larger  $k$  require larger networks, and this network is growing, but as hubs have a strong impact on their dynamics. This effect does not result from the nature of the half-chaotic network.

Removing of nodes is a different rule than the creation of sf and ss networks, so you can expect to break the distribution of  $P(k)$ , which defines these networks.

As you can see on the right in (a) and (b), where the distribution is roughly represented on the log-log graph, the removing did not spoil the sf (scale-free) network

The distribution for the ss (single scale) network (d) is slightly convex on the log graph, and with the removing (si in c) - a slightly concave straight line. In addition, in both networks (sh and si) appears as a result of removing  $k = 0$  (see Fig.1d)

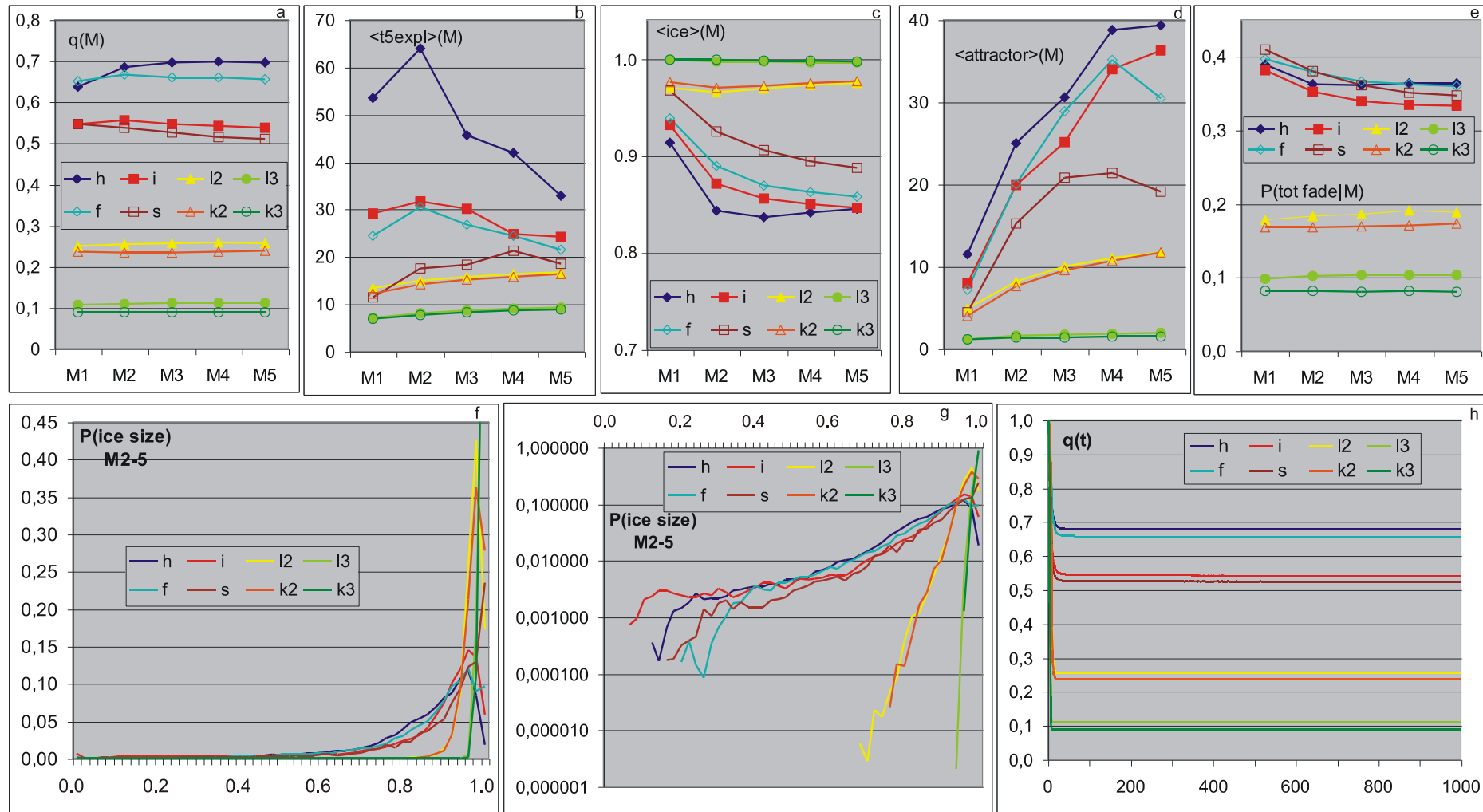


**Fig.4. Basic characteristics of the accumulation process** presented for the basic series in the met8 - 600 network with a threshold 0.2N.

**(a) -  $q(M)$**  shows the stability of the obtained  $q$  – degree of order during the accumulation of changes (see Fig.2d where it is also shown for threshold 0.5N).

**(h) -  $q(t)$**  is a sufficient basis for recognizing that the selected tmx was not too short (as it turned out in met2).

**(b) - average time  $t$  of the five latest explosions to chaos.** For tmx=1000 this indicates the statistical end of the explosion at the very beginning of the tmx interval (see Fig.2f and crocodiles Fig.6).

**(c) - medium ice in M dependence.** Only for the ss network the ice level decreases to the end of the examined growth, but the speed of this decreasing is not disturbing. The ice scale due to the increase of N was presented as a share, not as a number of frozen nodes as for m5.Fig.19ab (see Fig.2e). On average, ice remains clearly over half (scale in (c and Fig.2e) starts from 0.7, i.e. clearly above the middle of the range).

**(f, g) the ice size distribution** for the networks sh, si, sf, ss is stretched almost to the entire interval, which is slightly different from the situation in met7 (m7.Fig.11) and clearly approaches the met5 for bf (m5.Fig.19a). In general, the image of ice is consistent with the prediction of a similar ro-modularity mechanism for initiation also in the form of nodes adding and removing.

**(d) - the average length of global attractor** for acceptable ini is long distance from tmx and belongs to non-randomly small values. For accumulated attractor $>6$  was forced, but for the si, al and ak networks it was a problem, as many times we had to waive from this restriction (after 60 attempts to find an accepted with too small an attractor). Simulations of the k3 and l3 network would not have a chance of reaching  $N = 550$  if they did not allow for to waive from this limitation, which was aimed to evolving from the trivial starting PAS state.

**(e) - probability of permanent expiration to  $A1 = 0$**  without secondary initiations, which here have a clearly different character (see Ch.8.3.3). An important element in the assessment of the half-chaos maintenance mechanism.

### 8.3.2 Fade out and secondary initiations

Secondary initiations invoked in an unchanged structure in met1-7 by permanent point change of a function which during the process encountered again this unique input state are a much simpler phenomenon than in met8, where the structure changes and such a change causes something like a secondary initiation. In order to compare the number  $A1(t)$  of differing states of nodes, nodes added or removed are not included, but they function in structures - added in the disturbed and removed in the pattern. While in met1-7 after reaching  $A1=0$  it was possible to be sure that the new initiation is encountered by node with the changed function of this unique state of its inputs (point) for which the function has been changed, now  $A1(t)=0$  applicable not the entire reference and disturbed network, and node has many inputs and sends a result not related to the pattern (sf, ss, sh, si - on 1 link, ak, al on K links). Expiration to  $A=0$  is quite large, which can be seen on the crocodiles (Fig.6), and the general picture of the mechanism of maintaining a large  $q$  is very similar to the ro-modularity and based on the similar presence of ice (Fig.2e, 4cfg, 9e2-h2, f3, h3).

Due to the frequent occurrence of multiple threshold overruns and the appearance of PAS even above the threshold, which was not observed before, a few additional values were added for subsequent ini in the study of secondary ini and expiration. They are presented in Table 1. There are systematic differences compared to met5 and met6, but overall the picture is more similar to the model c from met5 than to met6. After the later ini than ini2 (third and subsequent), the expiration to  $A1=0$  drastically prevails in all met8, 7, and 5.

The similarity of the time distributions to the explosion (Fig.5) from the first (Fig.5a), the second (Fig.5b) and the third one (Fig.5c) suggests a similar mechanism of reaction to the secondary ini to the reaction to the first ini. The mechanism of these secondary ini is however diverse and complex. Generally, the secondary ini in met8 is to re-activate the changed area of the structure, easier to understand if it is a frozen area in the meantime (during  $A1(t)=0$ ). But not every such stimulation must result in a new avalanche of damage, and obtaining  $A1(t)=0$  does not necessarily mean freezing this changed area.

A significant difference to the image obtained in met7, 6 and 5 is the number of ini3, here significantly lower than ini2. This is clearly seen in Table 1 and also in Fig.5d. As before, the majority of ini3 expires, however earlier most of ini2 went to ini3, but now no longer. The differences between the time from ini to expiration does not help much in understanding, because it is exponentially decreasing. Measuring the time between consecutive ini is difficult to define and to obtain, because they can occur before the previous damage expires. For the above-mentioned reasons, defining such a moment is significantly more difficult than in met1-7. It is not advisable to repeat here the detailed observations contained in the description of Table 1, they form a general, very complex picture, which, despite differences, is sufficiently close to the ro-modularity observed in met5 and met7.

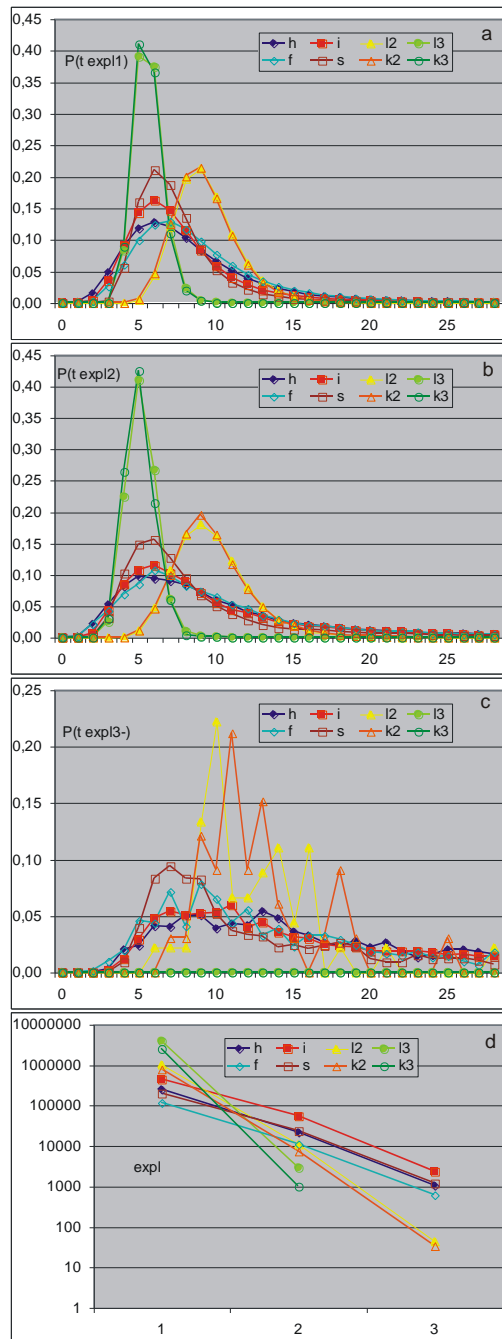


**Fig.5. Distribution of time to explosion** (basic series, threshold  $0.2N$ , 600 networks) **from ini:** first (a), second (b) and third and further (c). (Compare [m7.Fig.6g.](#)) The similarity of these distributions suggests a similar mechanism of reaction to secondary ini to the first ini. In order to justify the fluctuation on (c), the number of explosions that gave results (a, b, c) is shown in (d) (arguments 1,2,3, respectively). For ak3 and al3 there were no cases of explosion after ini3 and for ak2 and al2 there were only 33 and 45 respectively. It should be remembered that the secondary initiations in met8 do not result from encountering the input state for which the node function was changed during ini1, but they result from a change in the structure of the network after adding or removing the node and different than that in the pattern the function of this network section, whereas for comparison with the pattern, into A1 is not included the node removed present in the pattern. The same is true with the added nodes whose state is not taken into account when determining A1. The number of ini3 is significantly lower than ini2, which clearly distinguishes these results from those obtained in met7, 6 and 5. This is also shown in [Table 1](#).

**Table 1. Results of expiration statistics and secondary ini.** From the left: results for stage M1 for sh, then network sh, si, al2, al3 sf, ss, ak2, ak3 in the scope of stages M2 to M5. On the right for comparison, [m6.tab.2](#) is quoted, where the main reference is cfM and crM from met5, then the results are met6. Vertically from top 3 similar data sets: 1- after the first ini; 2- after the second ini; 3 - after the third and further ini, where ini consists in exiting the state  $A = 0$ . The table is supplemented with the values  $q$  and  $c=1-q$  already shown in [Fig.1d](#) and [m6.Fig.2d](#).

In the range of the description of the effects of the consecutive ini they are from the top: the share of the explosion into chaos and saved - means that ended with expiration to  $A1=0$  (fade) or reached  $tmx$  with  $A3 \leq \text{threshold}$  (other). PAS can appear in each of these categories. PAS\_c is within chaos, above the threshold, i.e. after the explosion into chaos. The remaining PAS cases are saved as follows: PAS\_f in the range of fade, and PAS\_o in the range of other. Total\_fade1 is the fade1 part - these did not meet the secondary ini up to  $tmx$ . Other fade1 encountered ini2. The division of PAS1\_f into tot.fade1 and ini2 is not known and is not obvious, because A1 is the difference between the pattern, which is usually not PAS, and the examined process, which can be PAS.

The division of fade2 is also poorly known, because ini3 there are third and subsequent initiations, and there can be many, so **ini3 is many times of fade2**, although the fade2 part also expires without further ini.

Both processes ending with  $A3 > \text{threshold}$ , i.e. classified as expl, can visit the order after the explosion ( $vi_o$  - order) under the threshold (especially often sh, ss and si after the first ini, but for sh and si this frequency grows strongly after secondary ini), and saved can visit chaos ( $vi_c$ ) above the threshold (here also sh after ini1, but after the next ini the frequency is decreasing).

As you can see, in met8 and met6 most saved1 is fade1, most of which has a secondary ini2. In met8 ini2 it usually explodes, only for sh and sf clearly, and for si it negligibly prevails saved2, while in met5 and 6 it radically prevails saved2 and in it fade2, similarly after ini3. In met8, usually saved2 is roughly half-divided between other2 and fade2, only k3 has other2 especially large due to the large share of PAS allowed from necessity (after crossing 60 akc with too small attractor). After later ini than ini2, fade3 in all met8, 7 and 5 is radically predominant.

Despite some differences, the picture is generally more similar to the model c from met5 than to met6.

35,057	28,568	40,814	73,625	88,867	31,054	42,816	75,754	91,207	expl1	%ini1	1	77,69	91,52	66,19	72,10	85,09	89,17
64,943	71,432	59,186	26,375	11,133	68,946	57,184	24,246	8,793	saved1	%ini1		22,31	8,48	33,81	27,90	14,91	10,83
1,020	1,330	0,741	0,001	0,000	0,784	0,368	0,001	0,000	vi1_o	%expl1							
0,129	0,033	0,004	0,000	0,000	0,008	0,000	0,000	0,000	PAS1_c	%expl1							
32,113	1,702	5,466	16,391	77,735	8,797	21,363	27,216	88,286	PAS1	%saved1		2,73	1,85	0,000	0,000	0,000	0,000
69,662	65,655	76,829	75,803	92,886	66,720	79,805	75,031	92,446	fade1	%saved1		10,75	17,00	99,99	99,99	100,00	100,00
30,338	34,345	23,171	24,197	7,114	33,280	20,195	24,969	7,554	other1	%saved1		86,52	81,16	0,011	0,006	0,000	0,001
0,538	0,371	0,172	0,000	0,000	0,257	0,095	0,000	0,000	vi1_c	%saved1							
0,217	0,773	0,049	0,000	0,000	0,040	0,000	0,000	0,000	c	%PAS1							
68,143	41,233	67,506	71,893	92,761	60,763	76,414	72,513	92,394	f	%PAS1							
31,545	57,751	32,428	28,107	7,239	39,170	23,584	27,487	7,606	o	%PAS1							
31,481	1,078	4,805	15,546	77,630	8,014	20,456	26,303	88,236	PAS1_f	%fade1							
85,877	77,285	74,707	93,379	99,116	79,731	78,819	93,432	99,418	tot.fade1	%fade1		43,66	58,96	0,00	0,00	0,00	0,00
25,417	23,241	43,155	57,030	70,454	32,053	53,116	59,345	75,655	expl2	%ini2	2	1,35	0,27	14,64	21,00	12,60	20,53
74,583	76,759	56,845	42,970	29,546	67,947	46,884	40,655	24,345	saved2	%ini2		98,65	99,73	85,36	79,00	87,40	79,47
4,811	6,083	3,896	0,019	0,000	3,707	2,276	0,000	0,000	vi2_o	%expl2							
0,027	0,046	0,004	0,000	0,000	0,000	0,000	0,000	0,000	PAS2_c	%expl2							
3,470	1,156	1,364	8,953	4,191	1,009	1,017	9,210	5,063	PAS2	%saved2		0,132	0,063	0,000	0,000	0,000	0,000
77,688	76,125	77,016	79,631	94,741	73,745	80,368	78,067	93,987	fade2	%saved2		93,49	86,99	100,00	100,00	100,00	100,00
22,312	23,875	22,984	20,369	5,259	26,255	19,632	21,933	6,013	other2	%saved2		6,383	12,947	0,001	0,001	0,000	0,000
2,228	1,336	0,884	0,000	0,000	1,031	0,691	0,000	0,000	vi2_c	%saved2							
0,260	1,193	0,207	0,000	0,000	0,000	0,000	0,000	0,000	c	%PAS2							
0,521	0,000	0,000	0,000	0,000	0,000	0,000	0,000	0,000	f	%PAS2							
95,833	98,807	99,690	100,000	100,000	99,153	100,000	100,000	100,000	o	%PAS2							
0,006	0,001	0,001	0,012	0,060	0,000	0,001	0,009	0,032	PAS2_f	%fade2							
170	166	154	152	236	158	143	148	213	ini3	*fade2		167	202	53	53	55	53
h M1	h	i	l2	l3	f	s	k2	k3	M2-5			cfM	crM	6fN	6fM	6rN	6rM
0,007	0,012	0,028	0,005	0,000	0,022	0,049	0,006	0,007	expl3	%ini3	3	0,000	0,000	0,026	0,040	0,011	0,019
99,993	99,988	99,972	99,995	100,000	99,978	99,951	99,994	99,993	saved3	%ini3		100,00	100,00	99,97	99,96	99,99	99,98
21,101	31,404	18,734	0,000	0,000	15,309	15,029	0,000	21,101	vi3_o	%expl3							
0,000	0,095	0,000	0,000	0,000	0,000	0,000	0,000	0,000	PAS3_c	%expl3							
0,028	0,003	0,005	0,075	0,252	0,002	0,004	0,069	0,028	PAS3	%saved3		0,026	0,035	0,000	0,000	0,000	0,000
99,629	99,628	99,603	99,549	99,685	99,622	99,596	99,542	99,629	fade3	%saved3		99,66	99,71	99,95	99,95	99,97	99,98
0,371	0,372	0,397	0,451	0,315	0,378	0,404	0,458	0,371	other3	%saved3		0,318	0,252	0,052	0,048	0,028	0,024
0,005	0,002	0,002	0,000	0,000	0,002	0,002	0,000	0,005	vi3_c	%saved3							
0,000	0,403	0,000	0,000	0,000	0,000	0,000	0,000	0,000	c	%PAS3							
21,602	20,161	17,571	16,621	23,650	14,706	15,294	12,438	21,602	f	%PAS3							
78,398	79,435	82,429	83,379	76,350	85,294	84,706	87,562	78,398	o	%PAS3							
0,006	0,001	0,001	0,012	0,060	0,000	0,001	0,009	0,006	PAS3_f	%fade3							
	0,693	0,545	0,256	0,111	0,661	0,521	0,235	0,088	rys.1d		q	0,355	0,171		0,254		0,125
	0,307	0,455	0,744	0,889	0,339	0,479	0,765	0,912			c	0,645	0,829		0,746		0,875

### 8.3.3 Observations of crocodiles

**Fig.6. Examples of 'crocodiles' and their elements.**

As in m5.Fig.7 the next pages of this figure are marking by letter, and within the page by digit.

Basic elements from top to bottom in sequence:

Growth in a given pass for consecutive 50 nodes. In the vertical line between the green line (the initial number of nodes= $N-50$ ) and the black one at the top ( $N$  as below at the upper left corner of the main rectangle) is 50 pixels. The horizontal axis is the consecutive attempts.

Red points indicate PAS. 2 pixels above the line in green, acceptable cases are marked, but with too small attractor for accumulation. Even higher by 1 pixel, at the beetroot marked change of the attractor.

Below, in blue between green lines ice is marked in scale 50 for accumulated cases. Below the second green line, to down in scale 50 are the numbers of nodes of  $k$ , ( $k$  = number of outputs from the nodes), for  $k = 0$  (black),  $k = 1$  (red) and  $k = 2$  (beetroot).

Showing these process parameters allows us to check how much ice and  $k$  are related to the growth. Generally, it turns out that it is negligible impact.

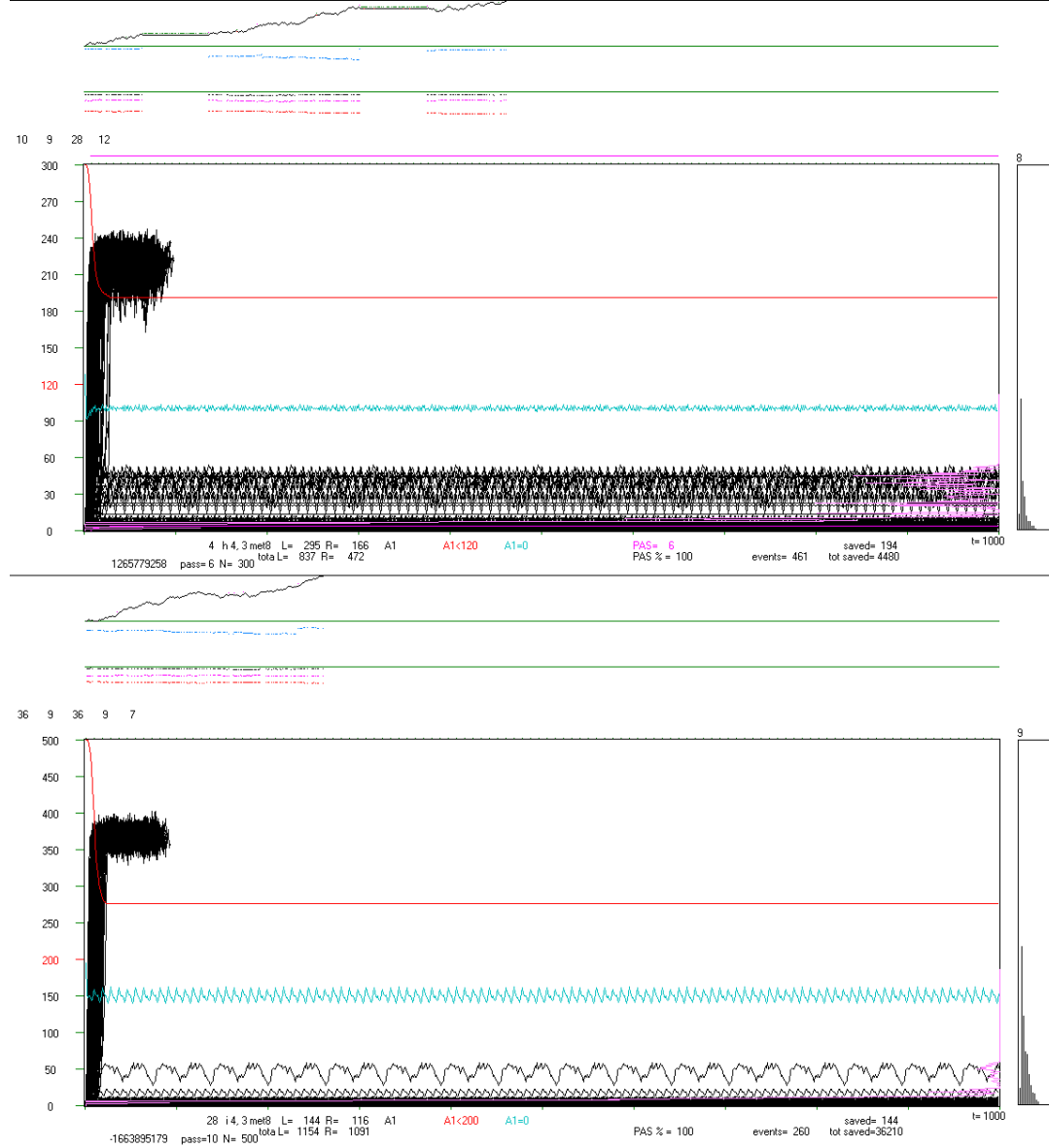
Even above the black rectangle of  $A1(t)$  from the left consecutive attractors are given numerically. Directly above the rectangle's frame, the occurrence of the  $tmx$  state in the initial pattern is marked in green, i.e. its attractor, also indicated by the number on the right. Between the attractors and the frame, the PAS range not differing from the pattern was marked, i.e. with  $A1=0$  (see b3) and additionally when PAS and a pixel above it when  $A1$  was above the threshold (b, c).

Below, in the rectangle, runs  $A1(t)$  (black). After going into chaos (above the threshold marked in red on the left, here are examples from the initial simulations where the threshold =  $0.4N$ , but the main simulation the threshold =  $0.2N$  and additional =  $0.5N$ ) only 70 counted steps of time  $t$  are marked (horizontal axis, 1 pixel = 1 step  $t$ ) but if at that time the process returned under the threshold, then it was counted on (see chapter 8.3.3 and c). Counted to  $tmx = 1000$ .

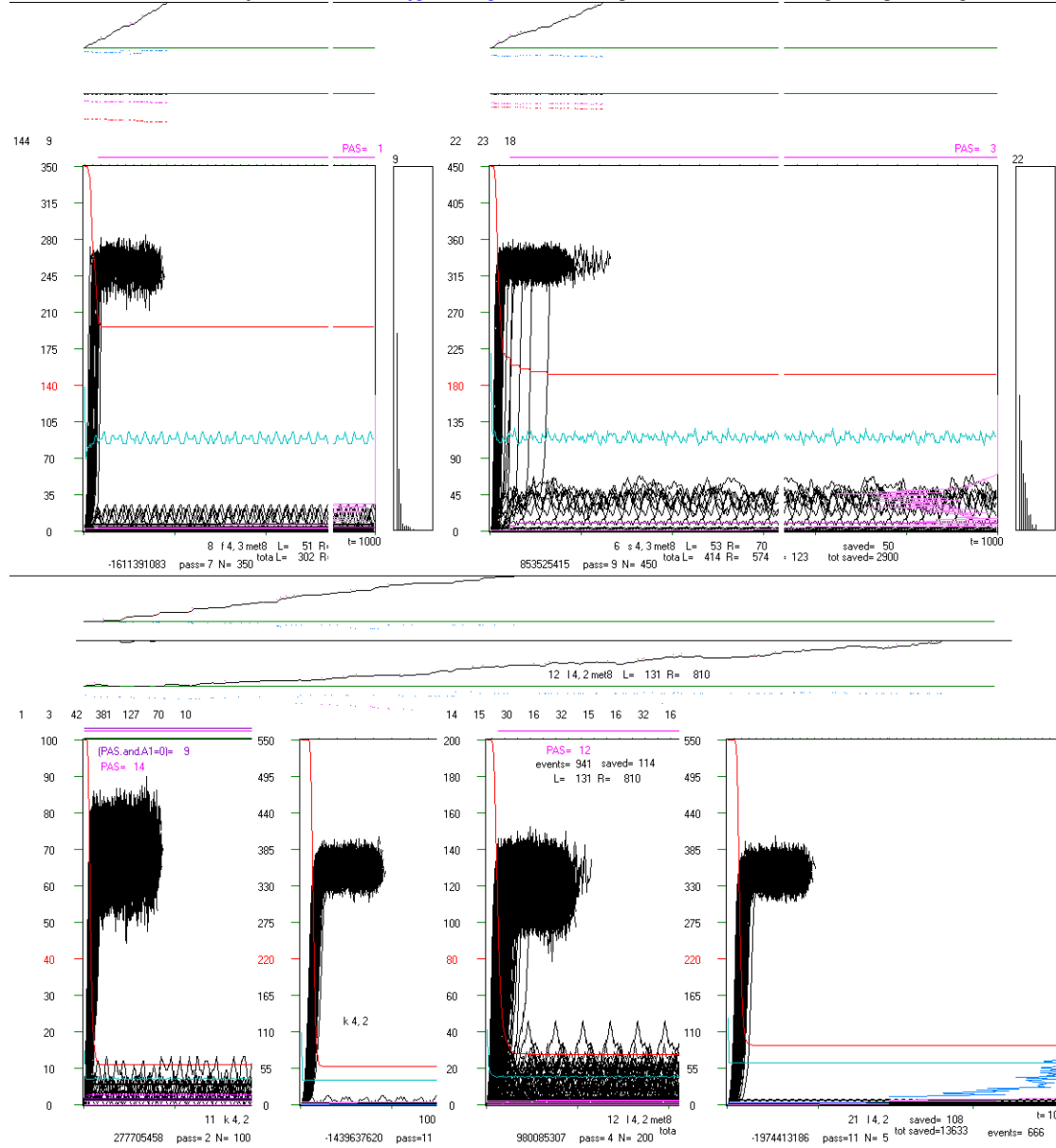
The scale on the left refers to the end of the pass, which starts from  $N-50$ . The  $A1(t)$  values are scaled:  $A1/N_{current} * N_{termin}$ .

The red line is  $q(t)$  summarizing the pass in scale  $q=1$  for  $N$ -terminal. Similarly, the blue line indicating the share  $A1=0$ .

On the right, the distribution  $P(k)$  for  $k=0$  to  $k=10$ , however (without normalization) the height in pixels is the number of nodes with such  $k$ .



(a) - Typical view of crocodile of the main types of networks in met8. (a1) - The sh network (it is a sf network with 30% removing of nodes and 70% addition of nodes as initiations). Here is the 4th network h of s,  $K=4,3$ , pass=6 (pass\*50= $N_{terminal}$ , here=300). ATTENTION: in the analysis of the results shown in Fig.1-2, the M stages are the sum of two consecutive visible passes here, so the M1 is an increase from 50 to 150, i.e. the passes marked on crocodiles as 2 and 3. (a2) - 28 network si, pass=10, also s,  $K=4,3$  as in the basic networks tested in met8: h, i, f, s.



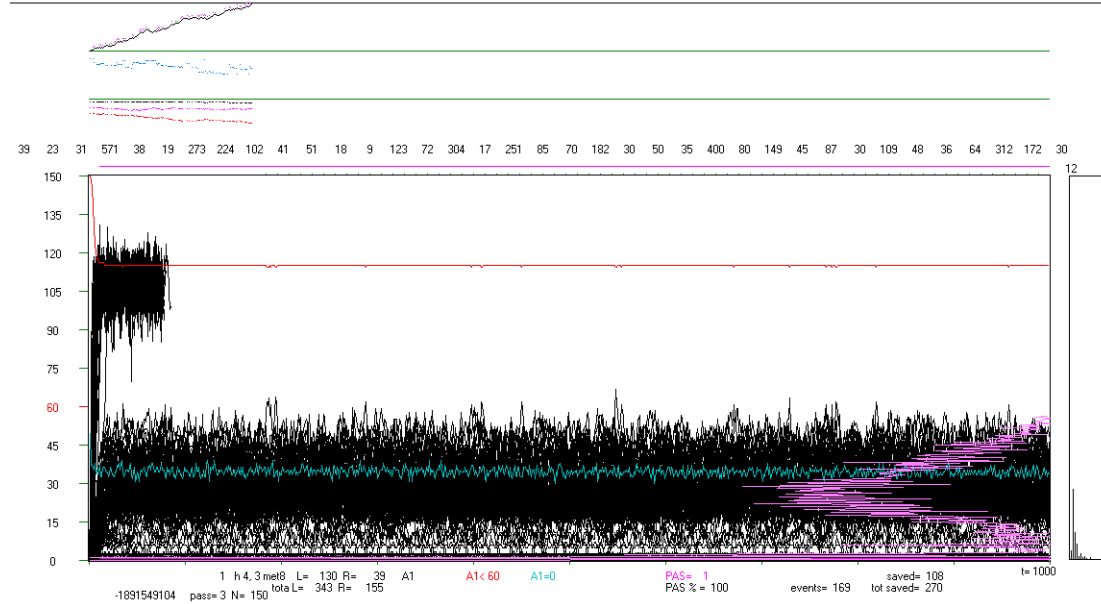
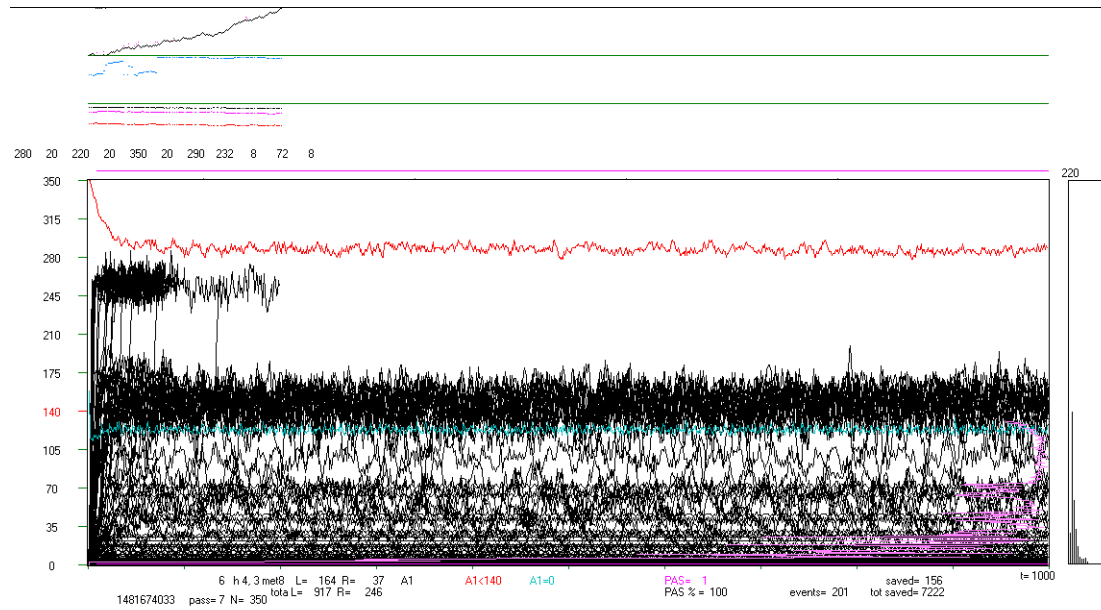
(b) - Typical crocodile images for other networks in the form of their most important slices. Of course, crocodiles are quite diverse, mainly the shape and width of the lower belt changes. Top row - net with  $s, K = 4, 3$  without removals: (1) sf 4,3 from the left and (2) ss 4,3 on the right. The cut out middle parts look like the range shown.

At the bottom  $s, K=4, 2$ , 2 examples of net ak 4,2 (3,4) without removals and 2 al 4,2 (5,6) with 10% subtraction of nodes. There was no sense to show  $P(k)$ , since the number of outputs from each node is  $k=K$ . Due to the lack of  $k=1$  and  $k=2$  for ak with  $K=3$ , used in the other tested types, the growth was much more difficult, which initially resulted in a reduction in removing up to 10%. It help too less, then we waive from  $K=3$  and adopt of  $k=K=2$ . Nevertheless, not all the passes of the al network managed to raise  $N$  by 50 on the 1000 test period and were stopped. Further 9000 attempts were allowed, and in this respect, also ak and al 4,3 were increasing by 50. Finally, after 200 consecutive trials, which did not allow accumulation due to too small an attractor, the accumulation of the currently proposed acceptable case was done regardless of its attractor. Growth and ice for (b5) was pasted into a place where normally the number of nodes with  $k=0, 1, 2$  was shown. Important information from the omitted areas was copied to other places. For (b4) and (b6) no growth was shown, there were no new attractors or PAS in these cases.

All the cases presented here are typical, they have a typical image for half-chaos observed earlier (met1-7) for initiation by permanent point change of function.

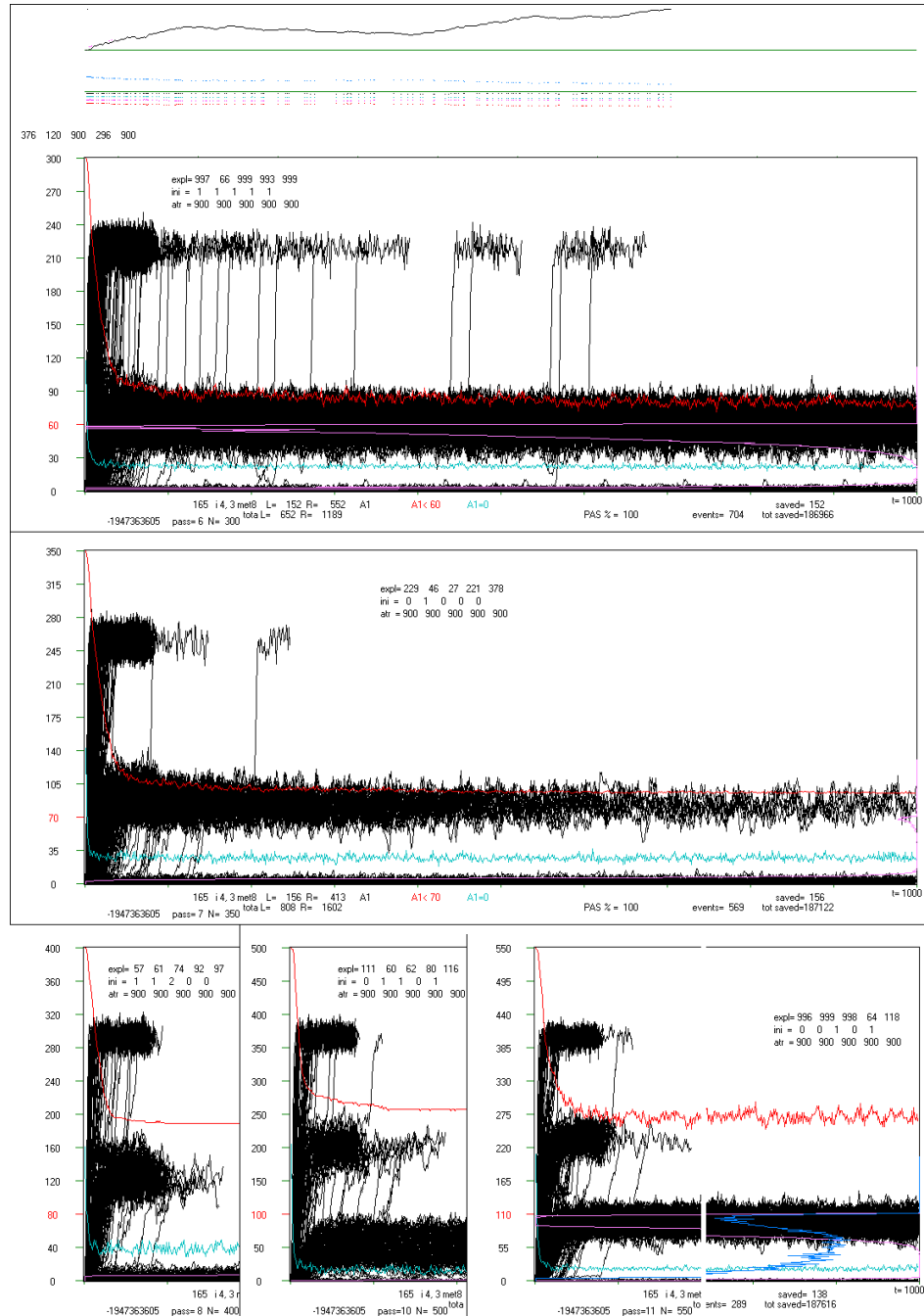
On the right side of the rectangle of  $A1(t)$ , on its right side, in each pass the share of  $A1$  below the threshold is marked in beetroot color. See also (c2). This method was already used in m3.Fig.3, and in m5.Fig.9 to show the presence of ro-modules. Here on (b2) and (a1) you can see a clear level more blurred black by  $A1(t)$  and indicated at the moment of the pass summary by the graph on the right side. In the last pass (=11), similarly as in previous studies, a graph for the entire accumulation process was collected in blue. Here it is visible on (b6), however, such imaging has proved ineffective (d5). Much more convincing is the indication of the size

of the ice (here b1,2 in general: Fig.4cfg, 9e2-h2, f3, h3), which remains at a high level, which indicates the mechanism of ro-modularity.



(c) – Less typical network cases h 4,3 (from initial series of simulations) in which there are quite high additional 'Derrida levels' (see chapter 8.4.2) suggesting the presence of large ro-modules (or modules). At the same time, there are a lot of attractors here. Nevertheless, the ice is kept at a relatively high level, and even in the case of (c1) it returns to very high values. These large ro-modules therefore froze similarly as it was observed in met7, which indicates their ro-modular nature. Similar cases occur sporadically and it is rather the property of a given network, because the images in other passes of the same network also show a similar character (see d, f). (c1) - the hypothetical 'Derrida level' for the 'ro-module' here was almost exactly at the threshold, which is not at all low ( $0.4N$ ). In this situation, despite passing over the threshold, the process was not included in the chaos, because it managed to return before 70 steps back under the threshold, going both ways many times up to  $tmx$ . It is difficult to conclude on such basis what to do with the arbitrarily taken threshold, it seems that it should be lowered, but after such a decision the case (c2) would be in the same situation and there would be more such cases. Such cases are so exceptional that it does not significantly affect the statistical picture of phenomena and the threshold was chosen well, but cases such as (c1) led to "backfilling" the gap between peaks (Fig.1b, 2abc), thus weakening the natural criterion of identity and in ch.8.2.3 to consider recognition as chaotic cases that have passed above the threshold at least once.

(c2) - a large number of different attractors, with a large spread, testifies to the complexity of the phenomena that took place here. Nevertheless, in both cases (c1,2)  $q(t)$  remains at a high level, which indicates the evolutionary stability of the half-chaos occurring here. Comparing the degree of blackness of the central belt in (c1) with (c2), it can be said that this spectacular belt as Derrida level at the threshold level concerns a fairly small number of cases. Unfortunately, the frequency of use A1 on the right side does not reach this range. See also (d, e2,3, f1-8).



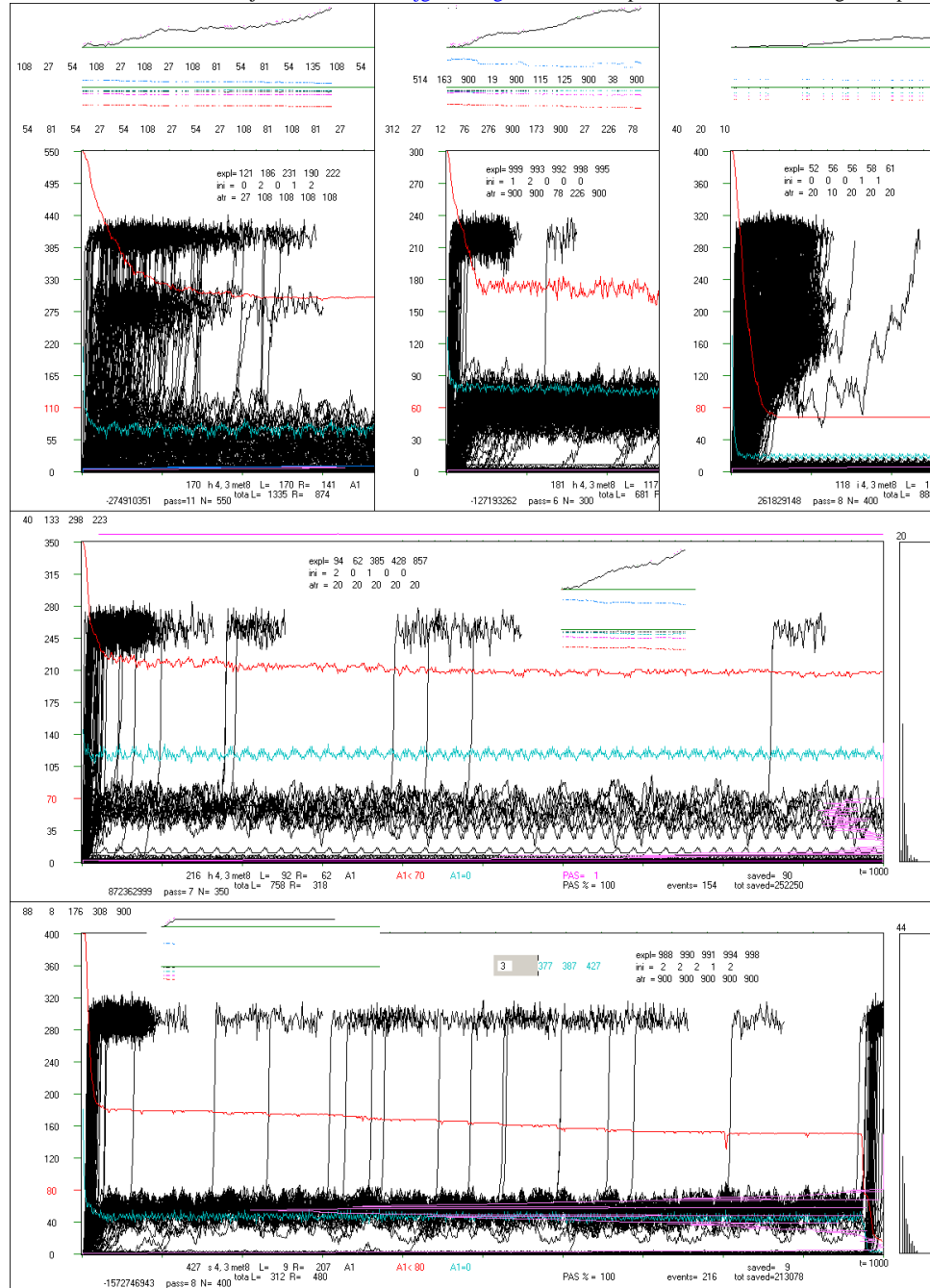
(d) – Similar to that shown in (c) network si case from the main series with a threshold  $0.2N$ . The history of the evolution of one network: 165 si 4,3 from pass 6, bypassing pass 9.

You can see here a characteristic increase in what we call a ro-module. In met8 these formations are not necessarily just "semi" modules, because the network is created under the control of a small change condition and real classic modules can be created - this possibility has been checked and this research is described in **ch.8.4.2**, and also in **ch.8.5** changing the original 'semi' to 'ro'.

It turns out that they are indeed classic modules, but not necessarily as a result of selection during evolution. When they are big and at the threshold, they are still growing in the positive feedback mechanism. These are sets of nodes with a particularly smaller than random number of links from it to the rest and a smaller average  $k$  - number of output links from the nodes. In this case, it is possible to suspect the participation of such "support". On (d1) you can see Derrida's level for a large module, almost exactly on the threshold (see Fig.11). Oscillations around this level do not allow to interrupt these processes, they form a characteristic toothed line  $q(t)$ , which, however, is relatively low. These oscillations mean that the 5 latest explosions concern the passage of a threshold within the belt of the excited ro-module, and not from it to the basic Derrida level for the entire network. The pattern started here with an unfound attractor (900) and the attractor usually remained large, which explains many late explosions.

In (d2) this ro-module, and maybe simultaneously the module, clearly grew more than the threshold and processes, which within the module went into chaos, most of the time remain above the threshold, so much of it is interrupted. This reduces the density of this belt over time  $t$  of the process.

Still the attractor is not found, but fewer processes will explode to main Derrida level for the entire network. In the next pass 8 (d3) the discussed module is already quite above the threshold, but at the bottom, the next such creation is born. It is still far from the threshold, it does not even reach it in pass 10 (d4) and it enters oscillations above the threshold only in the pass 11 (last d5). New ro-module (or module) significantly raises the level of  $q(t)$ . The mechanism of the phenomenon described here is examined in ch.8.4.4, but based on the ss network without removals, it explains why these modules are growing.



(e) Several other specific cases of the main series.

(e1) - two distinct Derrida levels in the field of chaos, which strongly suggests the presence of the module. Many attractors, the end of their enumeration inserted in the ice image range, which here is extremely small and stable. The truncated piece does not differ from the tip shown, as in all clipped cases.

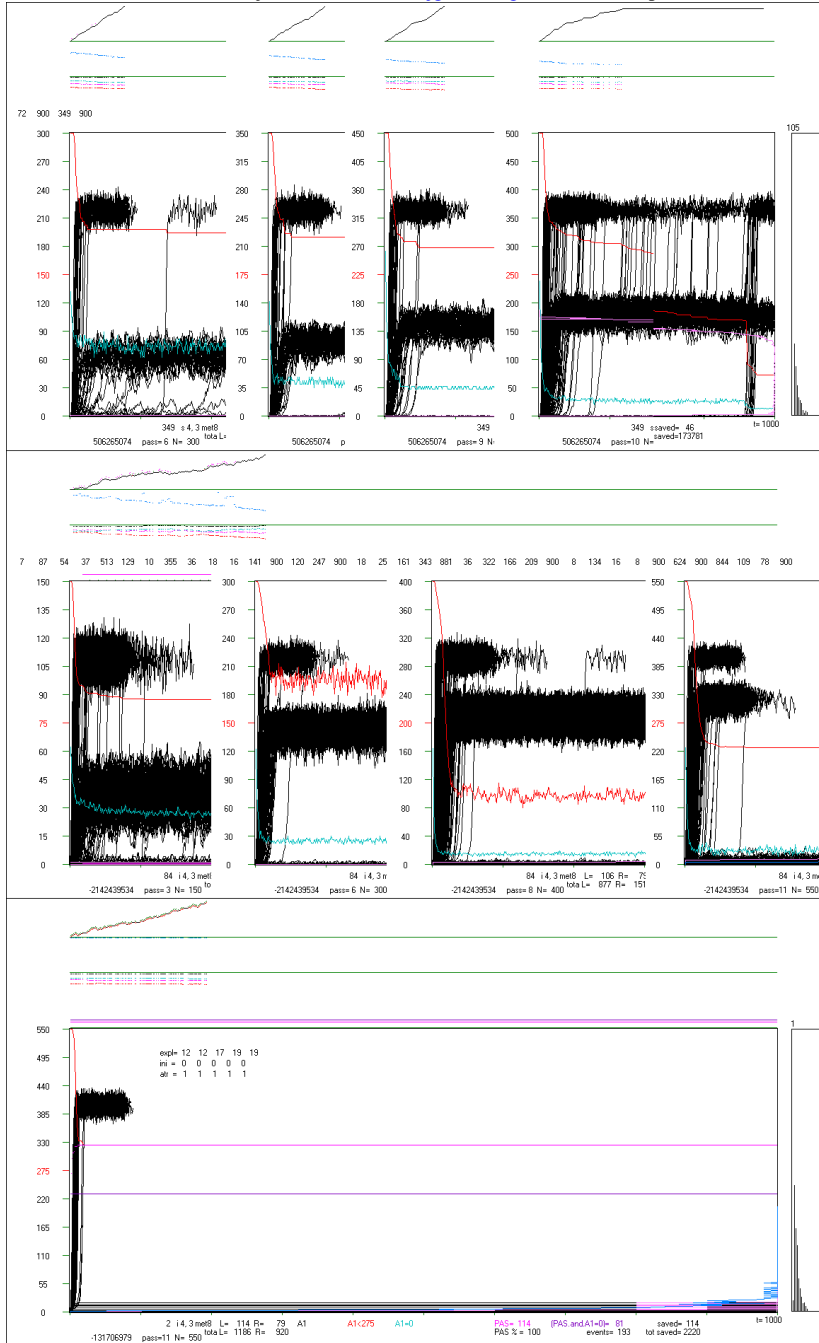
(e2) - probably the Derrida level in the ro-module on the threshold. Similarly, many attractors, but here at the end appears and attractor 900 - not found (rather, it is very large, but it could appear too late). Explosions do not stop until tmx itself, indicating the latest 5. It should be noted here that an explosion occurred at t = 992 at the attractor = 78. Also, the transitions from the lowest belt to the ro-module belt result from the lack of the second turn of the attractor.

(e3) - It seems that here, apart from the Derrida level for the whole network, there are also 2 (or more) lower levels in large modules.

(e4) - Despite the large attractors and not much ice, there was a PAS proposal, not accumulated due to too small attractor. The number of processes in the ro-module belt hooking the threshold is not large - these few explosions to the Derrida level of the entire network clearly thinned it. This image indicates a chaotic course in this belt, although it may be the result of a large or late attractor.

(e5) – One of the few cases of chaotic collapse as a result of pulling the "tail" with the explosion as a pattern. There were several such cases among 600 networks. When the attractor is not found in the tmx range, even for the accumulated chance of an explosion just after tmx, in the next 50 steps t, is significant. For these 50 steps the beginning - the moment of initiation is shifted and the end of the pattern is added. This end is not checked - it would require a checked pattern. The occurrence of such a large change in the pattern is equivalent to the accumulation of chaotic change as in experiment X in met7 - from this point the system is normally chaotic, not half-chaotic. The chances of a change in the opposite effect and with such a long delay are negligible. However, a similar situation in the pattern that would occur further than these 50 steps is no longer as dangerous as it is not in the tmx range after shifting and allows the accumulation of a "healthy" pattern, usually different at that point distant from the initiation point.

Such 'hauling of a chaotic tail' is often the result of the increase of the modules with the chaos inside and passing them through the threshold or a typical strong extension of the attractor or reaching it beyond the tmx.



(f) Specific examples from the series with a particularly high 0.5N threshold. The upper line (f1-4) shows the evolution of the 349 ss network 4,3 ended by collapse as in the case (e5) by pulling the tail of the pattern with a chaotic explosion. Despite the fact that the attractor left the tmx range already in pass 6, only in the pass 10 explosions to chaos occurred up to tmx. This increased the chance in the pass 10 for such an explosion on a stretch of 50 steps after tmx in accumulated case. Early passes ended the explosions much earlier and these uniform sections were cut out, in the pass 10 it was cut down in the middle part. Explosion in the pattern makes it practically impossible for the process to pass through to this place - this corresponds to the X experiments in met7. It should be noted that almost all later explosions are transitions from the middle bar to the basic Derrida level - in this pass it has a different character in this aspect than in the previous passes. However, after reaching the pattern break point, the processes from the A1 level in the range of a few will also explode. Since the adoption of such a pattern, not one has been accumulated by 160 trials.

The second line (f5-8) contains the case 84 si 4,3 close to (d), where the module grows faster than the threshold, but after passing it over the threshold, the network regains stability. Such a high level of Derrida balance indicates the size of the module, while the high level of q(t) indicates that the disturbances within this module can be accumulated. Data above the A1(t) rectangle - growth, ice, k0-3 number and subsequent attractors, are shown in the whole range only for (f5), the attractor was not detected (900). Such cases were the reason for undertaking the search for classical modularity in ch.8.4.4, where they were analyzed in the 'great' group, and the analysis of the case was started separately investigated 349 ss shown here in the top line (f1-4). Modularity has indeed been found and the black belts observed here are Derrida equilibrium levels in local clusters of a module nature. This does not mean a change of the ro-modularity mechanism to modularity, since the 'rest' is the ice, so both mechanisms work simultaneously in the same direction.

There is another crocodile (140 ss) of this type analyzed deeper in terms of modularity in Fig.11.

The last example (f9) 2 si is extreme in the opposite direction - all accumulated are only PAS, and the pattern is also PAS, although it is pass 11, and during the entire evolution it was tried to counteract the shrinking of the attractor.

## 8.4 Tendencies

Tendencies have already been defined in my doctorate in 1987 and later described in [krab, dgec, ggec], where it is the difference between a given random distribution and the distribution modified by the adaptation condition. Here, the equivalent of the condition of adaptation is a weaker acceptance condition based only on not exceeding the threshold of great change, but the modifying factor is the condition of accumulation, slightly stronger than acceptance (larger attractors than 6 to increase the strength of persuading the obtained results), because it maintains the particular, studied specificity of the system state called a half-chaos (although acceptance is enough). In general, any statistical differences in nodal properties resulting from the evolution that maintains half-chaos (controlled by a small change) are tendencies. For example, the tendencies are: the persistence of half-chaos and the persistence of a high level of ice after the start from the point attractor, which disappear immediately after allowing the accumulation of random changes.

### 8.4.1 Tendency of conservativeness of older nodes

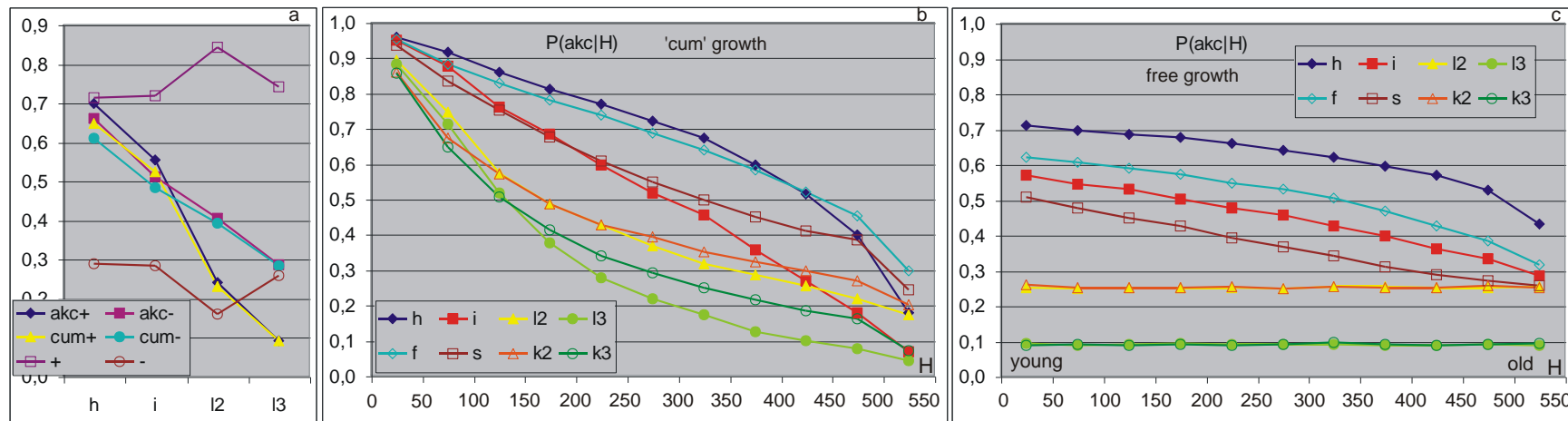


**Fig.7. The tendency of conservativeness of older nodes.**

(a) - Probability of acceptance and accumulation of random proposals for adding or removing the node and contribution of accumulation of adding and removing. As you can see, for all the changes have a much lower probability of acceptance and accumulation than in sh and si (always  $k=2$  (l2) or 3 (l3)), and the addition is much smaller than the removal. The share of subtraction in the change proposal is 0.3 for sh and si, and for al it had to be reduced to 0.1 so that the network would grow. Generally, acceptance and accumulation have a similar chance.

(b, c) - Probability  $P(akc|H)$  of acceptance of node removing for all 8 types of networks. For sh, si, al measurements during the last pass, for sf, ss, ak during an additional attempt to remove the nodes after reaching  $N = 550$ , without accumulation. Horizontal axis H - intervals of the sequence of the connection of the nodes corresponding to the "depth of history" and the "age" of the node. The 50 youngest among those currently present, joined in the last order, constitute the range 0-50, and the oldest 50 among currently present - range 500-550. (Fig.8 presents the measurements for each pass.)

(b) - for networks growing with a condition of accumulation. All networks show a clear relationship – for older nodes acceptance of removal is less probable.

(c) - for networks growing randomly without the condition of accumulation. Networks al, ak, which have fixed k do not show the dependence of the probability of removing acceptance from the age of the node, whereas the networks sf, ss without removing and sh, si with removing show such a relationship, although it is weaker than in (b). This suggests that the decrease in the chances of accepting the removal connected to the age of a node in the network ak growing with the accumulation condition results from this condition, and for the sf, ss, sh, and si networks also results from the increase of the degree k (number of outputs).

For al which for random growth (c) does not show dependence, the relationship in (b) is a demonstrated tendency of conservativeness of older nodes. For the other networks, this tendency is seen in the increase in slope at (b) relative to (c). Formally, (c) dependence on the age of the family is not a tendency (in my sense), because it does not result from the condition of accumulation.

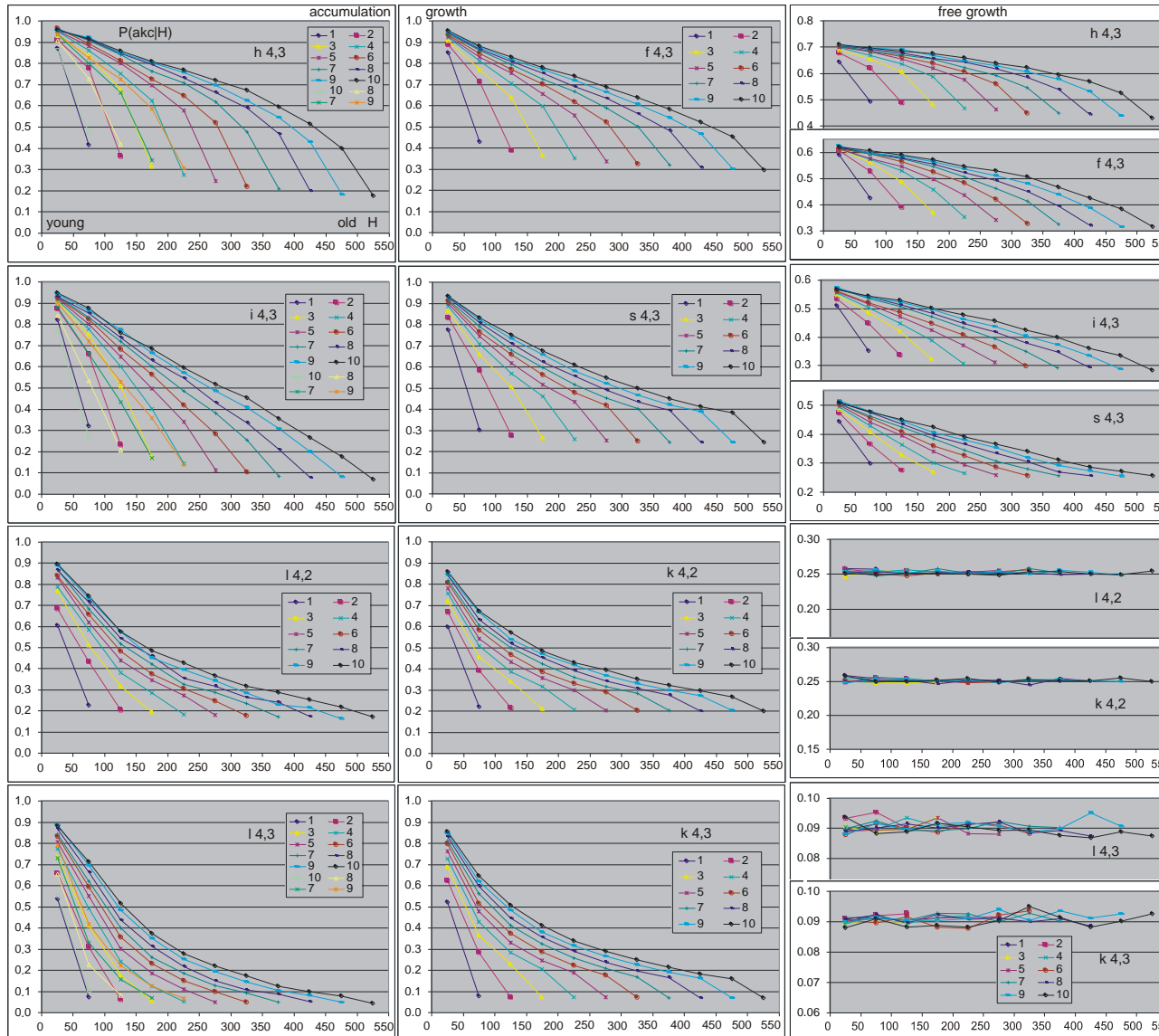


**Fig.8. Tendency of conservativeness of older nodes during network growth.**

$P(akc|-,H, pass)$  for growth with a condition (two left columns) and without accumulate condition (right column).  $H$  - connection order, age of the node. (See Fig.7). It turns out that the shape of these dependencies in the next passes is practically the same and after scaling lines overlap. Only the last interval has often little specificity. This property basically allows us to limit our self to the most accurate data from the last pass shown in Fig.7.

One can suspect that nodes, which are already in the network for a long time and have not been removed yet (in networks sh, si, al), are actually more difficult to remove because of their environment. This environment changes and maybe after some time from an ineffective attempt to remove, let it be removed. In cases of network sh and si a separate aspect is the gradual arrival of outputs in nodes during evolution, which, of course, makes removing more difficult, so only the al network is suitable for checking this hypothesis. Therefore, an additional measurement of the probability of accepting the removals was made depending on the sequence of connection of a given node to the network. There was no recorded time of residence of the nodes in the network, it was enough to divide the current set of nodes set in the order of connection (which was already ready) for the consecutive 50-elements sets..

The resignation from the acceptance conditions immediately creates a chaotic state, and in it  $P(akc|-,H)$  is practically 0 for each node, regardless

of when it was connected to the network. Therefore, it is not convenient to compare this result to an identical, completely random process, but you can examine processes similar enough to show the presence of tendency.

We can build a network randomly, after which, just like after the first pass, build a PAS state, and then examine the possibility of accepting the removing of each node without the accumulation of such changes. An indirect investigation may be a growth of sf, ss and ak networks, and after each pass a test  $P(akc|-,H)$  of all current nodes without accumulation. In this case, this tendency does not result from the "difficult" of node removing during the accumulation of removals.

Therefore, such tests have been done. Their results are shown briefly in Fig.7. and more specifically, taking into account the passes of growth in Fig.8. As expected, randomly created networks ak and al do not show the dependence of the probability of removing acceptance from the age of the node. It turns out that the sf, ss, and ak networks growing with the condition of accumulation also show the tendency of conservativeness of the old areas of their structure, i.e. a result of the condition of accumulation and not the exhaustion of nodes that are susceptible to removing. As can be read from Fig.7b, the strength of the tendency for networks with and without accumulation of removals is similar, but usually the removing slightly increases it. So we have as many as 3 independent mechanisms that create such dependence, because there is an increase in node degrees with the time of network growth (Fig.7c networks sf, ss, sh, si, however, this mechanism does not give a tendency in my sense). It should be noted that in the presented met8 studies there is not a condition of adaptation, but only a part of it. The condition of adaptation (more precisely, not reducing the degree of adaptation) in my earlier works [krab, dgec, ggec] was indicated as a source of a similar tendency. A similar phenomenon was initially observed as the regularity of evolution of ontogenesis - "terminal variability and conservativeness of early stages" that de Beer formulated in 1940. A similar but much more complex question about the resistance of old nodes to changes in the environment can be put forward (with a condition of small change maintaining the half-chaos) in processes without removing. Then the criterion of old age of the place would have to be assessed on the basis of the nearest neighbors. However, this was not undertaken in the presented work.

#### 8.4.2 Comparison of modularity effects

Allowing changes in the structure in met8 (because in met1-7 structure was constant) controlled by the condition of small change creates the possibility of emerging tendencies in the impact of the small change condition on the frequency of connections between subsets of network nodes, i.e. the effects of modularity. The lower belts in the 'order' range (under the threshold), under which there is clearance, were interpreted as a state of chaos (Derrida balance) in a range of growing module / ro-module. It was necessary to check whether it is only a ro-module or also a module. An easy indication of a set of nodes suspected of being a classic module makes it much easier to check.

The presence of removals causes large changes in the structure within one pass, and candidates for modules are easier to point under the threshold, so the case 'si 165' with the main threshold 0.2N shown in Fig.6d is less suitable for analysis, where it was planned to get a picture of the effects of modularity in subsequent passes, rather than the case of 'ss 349' with the threshold 0.5N shown in Fig.6f1-4, where connections in the pass range change slightly. Passes 5-9 were analyzed here, as in pass 10 there was a chaotic collapse, the reasons for which are not yet in pass 9, and clear, appropriate lower belts start in pass 5, in which the network is relatively large. The results of this analysis are shown in Fig.9a.

The black belt range clearly visible on the crocodile allowed to determine the set of nodes that have changed states relative to the pattern in a process that falls within the indicated range A1(t) in the section t from t=200 to t<sub>mx</sub> (later to 900 to cut off the collapse area in pass 11). (More accurately: A1 is found at time t in the given range, and such nodes are entered into the 'mo' set, which at the moment t+1 have a different state from the pattern, if the process ends with acceptance.) The set 'mo' is a hypothetical module. Of course, this is not an exact designation of the module, but well-approximated, sufficient to check the statistics of its connections.

These statistics very clearly indicate the presence of modules, but these are not strongly delimited modules. To detect unevenness of connections, measurements with predictions assuming no modules should be compared. The input links are fixed - each node has exactly K=3, but the output links, which are k, have many more possibilities of correlations. Fig.9a shows the basic correlations obtained from counting 4 sets of links: from mo (module) to res (rest); from mo to mo; from res to mo; from res to res. If there were no effects of modularity, the number of these sets should result from the shares of sets of mo and res. For example, the share of the input links of the set may be  $P(i_{mo})=mo/N$ . However, the number of output links in mo and res may not be as it appears from the size of these sets (i.e. the number of nodes in these sets), and it is not - in mo the node outputs is radically less - Fig.9a3 (averages k: <k>).

$P(o_{mo})=(\text{sum of the output links from mo})/(NK)$ . The expected shares are  $P(i,o)=P(i)*P(o)$  for the respective pair of sets mo and res. Such pictures are in the vertical 1 in Fig.9. In them the discrepancy of the measured shares with such predictions is visible, what is shown in summarized view in Fig.10. **The classic module is more strongly bound in the middle than with its neighbors, which is its essence, and such an image emerges from the presented measurements, which indicates the presence of classic modules and their relationship with the criterion of selecting the set of mo.**

In the vertical 2, Fig.9 the division of the output links from the mo and res to the inbred and to the opposite set is shown. It is  $P(i|o)$ , here the prediction is easy to determine P(i), because a priori can not be seen depending on where the link is from. The division of these links into both directions also turns out to be non-random. Fig.9a3 also shows the coefficient of damage propagation  $w=<k> (s-1)/s$  [dgec, it] resulting from <k>, allowing to predict system behavior, related to the **Lyapunov exponent**. The set of mo selected as 'more orderly' actually has this coefficient much closer to unity than res, especially for inbred links.

There is no need to repeat here the description of Fig.9, which discusses the research in detail. Further in Fig.9b a similar analysis of another similar case is shown, but already in the range of passes 4-11. It gave similar results, maybe not so radical for mo, but the differences resulted in the need for more statistics. Therefore, 7 selected

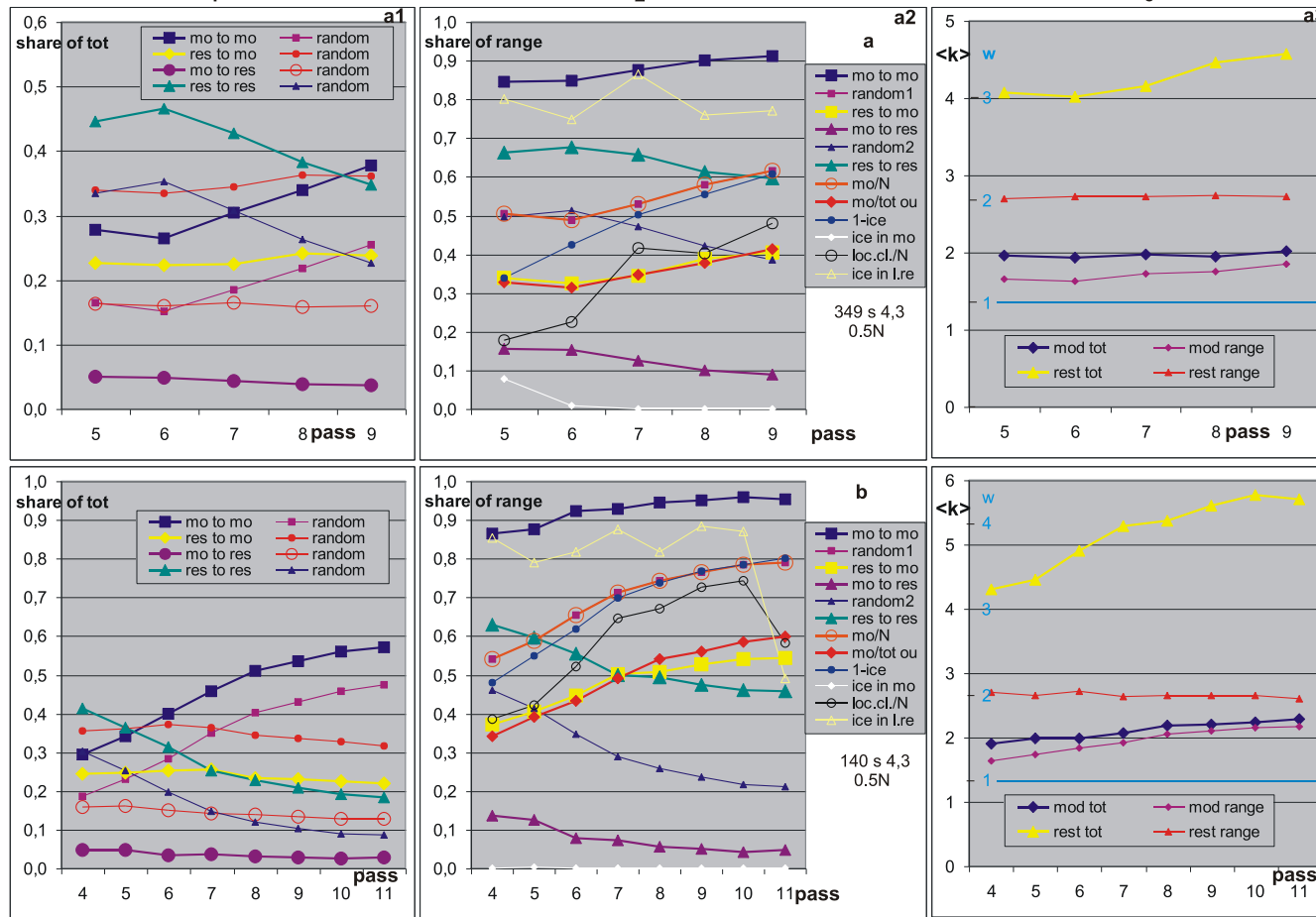


**Fig.9. Modularity effects in networks ss and sf, K=4,3 and ak s,K=4,2, threshold 0.5N.** The consecutive lines are marked by letters, usually they refer to separate measurements; verticals (always the same measurements except cd4, hnp3) - digits, which is marked above the top row (a).

**ab** - results of the analysis of **individual ss networks with particularly distinct modules in the chaotic state** visible in crocodiles. **a** - first analyzed case of the ss network selected from the main simulation with the threshold 0.5N, where it was the 319th network. This case is shown and described in Figs.6f1-4, 11. Passes 5-9 were analyzed, as in pass 10 there was a chaotic collapse.

The following **table** gives for 4 types of links

s349	1,2x	1y	1z	2y	2z
m>m	1,62	0,73	0,65	0,93	0,82
r>m	0,66	0,95	0,94	0,83	0,82
m>r	0,27	1,40	1,02	1,76	1,29
r>r	1,41	1,28	1,48	1,12	1,29
s140	1,2x	1y	1z	2y	2z
m>m	1,34	0,52	0,39	0,91	0,68
r>m	0,69	1,12	1,12	0,68	0,68
m>r	0,24	1,67	1,24	2,93	2,18
r>r	1,79	2,26	3,58	1,38	2,18

(mo to res = m>r); x=measurement/random; y=pass5/pass9 for measur.; z - for random.

For ss 140 it is pass4/pass11. For the presentation in the 1&2 columns x is obviously the same, for the experiments presented in c-p, this value is shown in Fig.10.

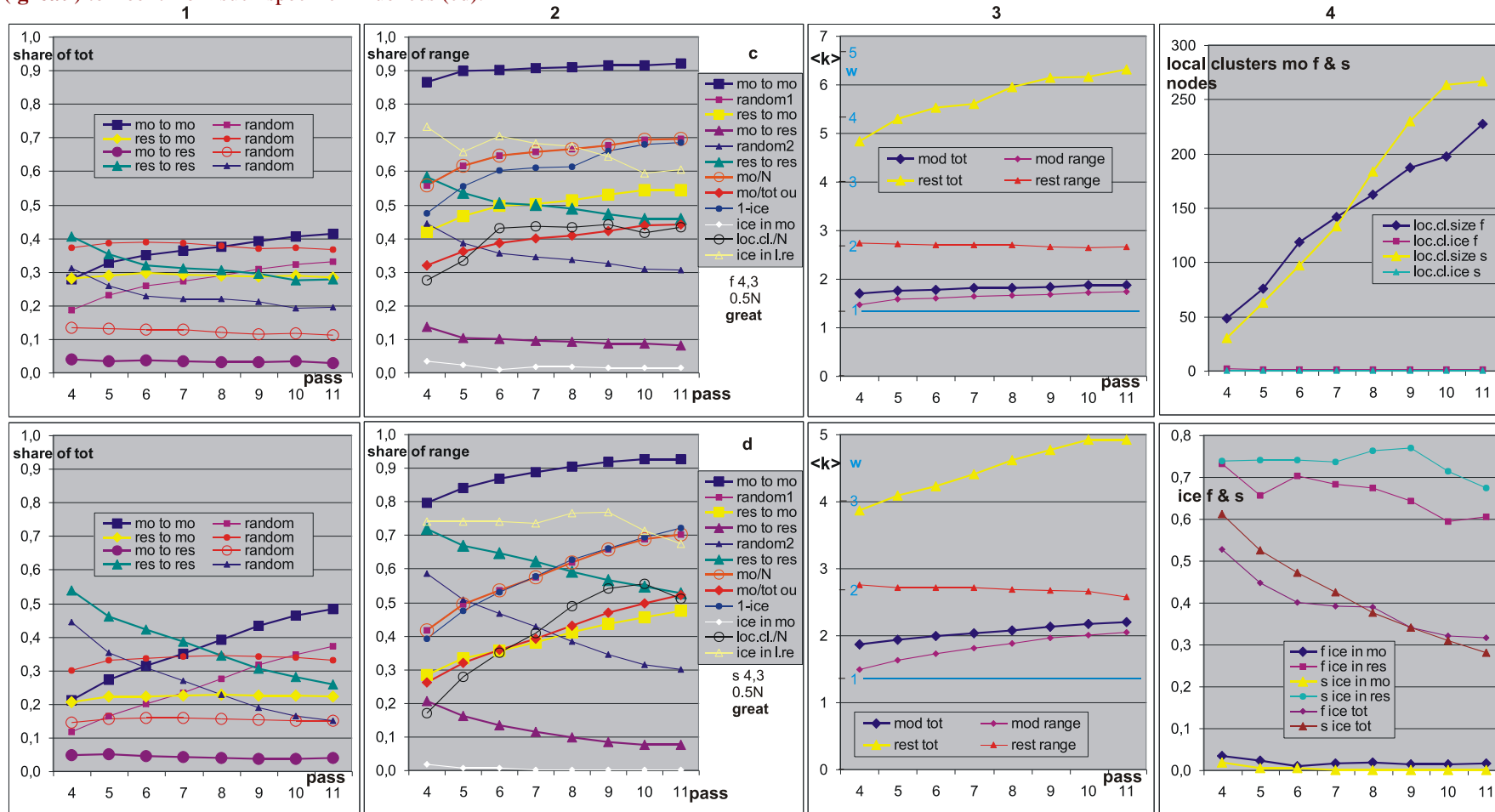
**a1** - share of 4 types of links in the set of links of the entire network at the end of the pass. Here 'random' =P(io)=P(i)\*P(o) (o=output from mo/res; i=input to mo/res) is prediction assuming no modular effects, resulting from: P(i) for inputs - from the size of **sets: mo (module) and res (rest)** - see a2 mo/N, because each node has K inputs; P(o) for outputs - from the summary of the number of outputs in mo and res, since <k> (see a3) turns out to be clearly different in these sets. Particularly **large deviations has the share of links from mo to res** - much smaller than expected (approximately 1/4 random, see table above). The remaining connections differ from the random by a factor of about 2/3. **Classic modules should have stronger connections inside the module, and weaker between, and here we are observing such a situation.**

**a2** - share of directions of output links in the range of sets mo and res; mo is less than half of the network nodes (mo/N), but has a small part of the output links (mo/tot). Here, random predictions = P(i|o) (e.g. random1=P(link to mo|output from mo or res)=mo/N) result from shares indicated by mo/N, then random1 coincides with mo/N and random2 is its reflection in 0.5, as well as other dependencies. Note: N grows in the pass by 50, but the set mo is defined at the end of the pass, whereby according to this, links are assigned to the corresponding sets according to their end and beginning. The largest and stable **deviation is mo to res** from random2 (of course, as in a1).

**a3** - average k in sets (tot) mo and res and part of these output links, which goes back to the range of these sets. The distance between tot and range is the part of tot that goes to the opposite set. <k> should be exactly K=3 and the network is autonomous. Because the coefficient of damage propagation [dgec, it]  $w=<k>(s-1)/s$  but here  $(s-1)/s=3/4$

It is enough to change the scale linearly and we have  $w$ , which has a simple relationship with the Lyapunov exponents. Inside the investigate module  $w$  is near 1, and in (egikmo3) below 1, i.e. in 'norm' and 'free' the set mo is ordered. The rest has a big  $w$ , but the damage did not get there and the area remained mainly in the form of ice (ice in loc.cl. res in vertical 2 and d4, hn3).

**b** - analogous analysis of a similar case of 140 ss (Fig.11), but in the range of passes 4-11. A lot of differences can be seen, mainly the increase in mo/N shown in b2, which in the case (a) was quite stable. This entails inclination in (b1). Basic deviations are, however, maintained. This indicates the need to get such an analysis from many cases ('great') to free it from such specific influences (cd).

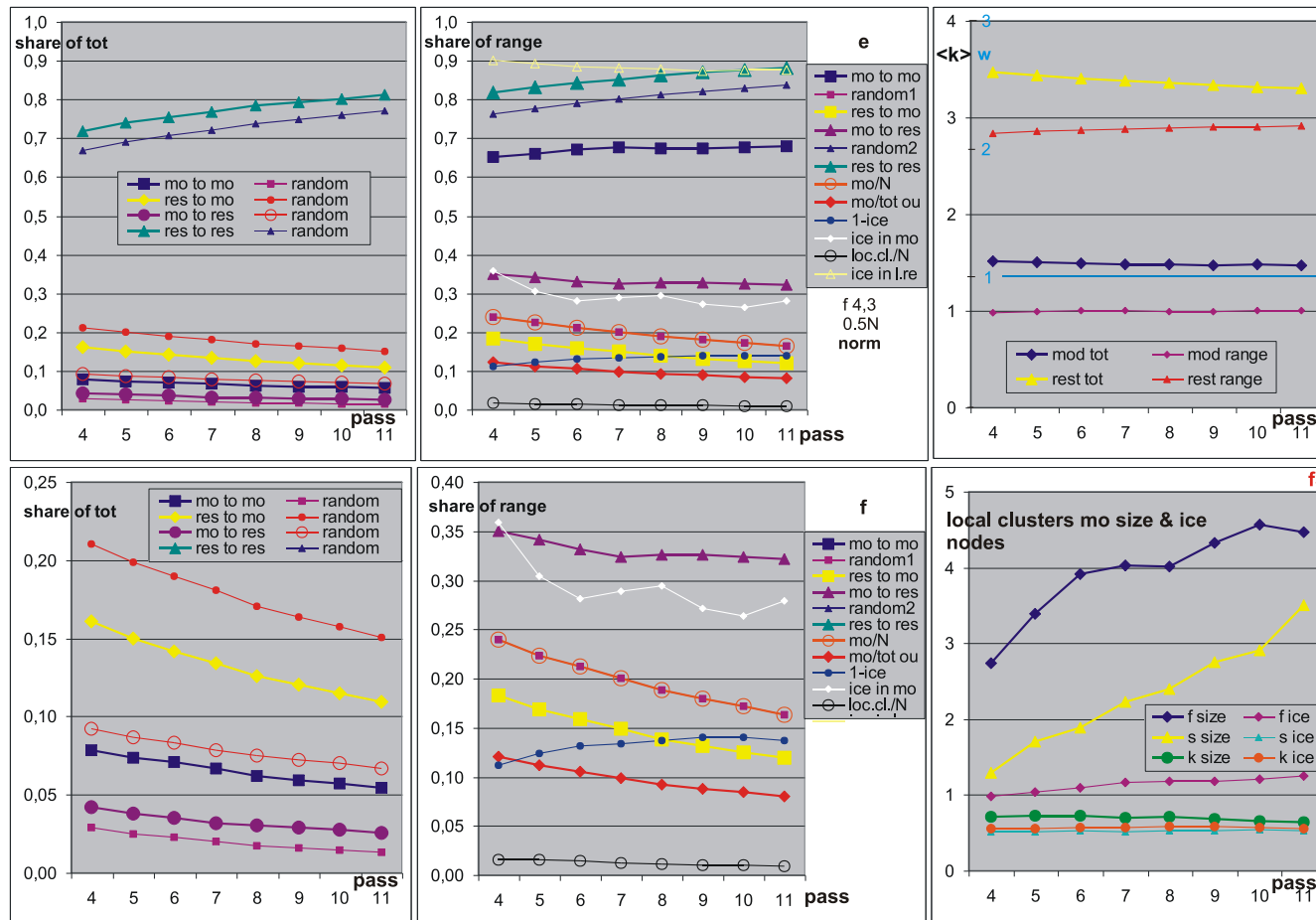


**c,d** - is a similar analysis, but the results are composed of **selected 7** networks, which creates a 'great' group in Fig.10. The results from each network, regardless of the size of the set mo, were added together with the same weight, i.e. the sum/7. Here, nets were selected that had a well separated belt A1(t) on the crocodile, similar to Derrida level, but significantly lower. These levels indeed correspond to the sizes of local clusters (2 - loc.cl/N, c4, see Fig.11) and the ice inside these clusters has actually disappeared (2 - ice in mo, c4, d4), but remained in res (2 - ice in loc.cl.res, c4, d4). This suggested a similar mechanism of its creation, i.e. a picture of chaos in a subset of set of nodes - a module from which somehow damage does not come. For each pass the range of this A1(t) was indicated. Mainly it was about cutting off processes with A1(t) close to 0, which are usually the most, but they can not be seen on the crocodile. It turned out, however, that such a limitation does not give clearly other results in the most important

7 sf	1,2x	1y	1z	2y	2z
m>m	1,46	0,67	0,56	0,94	0,80
r>m	0,76	0,99	1,02	0,77	0,80
m>r	0,27	1,39	1,19	1,67	1,45
r>r	1,52	1,46	1,61	1,27	1,45
7 ss	1,2x	1y	1z	2y	2z
m>m	1,59	0,44	0,31	0,86	0,59
r>m	0,67	0,91	0,90	0,60	0,59
m>r	0,27	1,28	0,96	2,74	1,96
r>r	1,56	2,09	2,96	1,36	1,96

aspects. In addition, this phenomenon was to be seen in the consecutive passes from 4 to the end. There were few such cases, often such a picture appears only in two to four passes and is much weaker (Figs.6c,e4,5, Fig.11, the right bottom for sf in another view). The results for both types of networks are similar - the main exceptions indicated above persist, but also the differences related to the type of network can be seen. These differences were systematically observed on the results visualized as in the case of 'b', they are not the result of strong deviations in individual networks.

For plots in vertical 2 'l-ice' was added. The interpretation of this value is exactly as in Fig.2e <ice>(M) and Fig.4c. It was supposed to show that the res set consists of ice and mo of active nodes. As you can see, mo "falls within the ice range", which indicates the problems of interpretation - the set may never work as a whole, as it was imagined at the beginning, in a particular process it is a local cluster. In the cases 'great' selected here this cluster has a size comparable to mo (c4), but for 'norm' and 'free' (el) it's a small part of mo (mainly fl3), the remain part='mo'-'loc.cl' is the ice in great part. We can not say what part of the mo is the ice, the ice can only be examined after completing one particular process and next averaging it. The set of mo is to indicate the

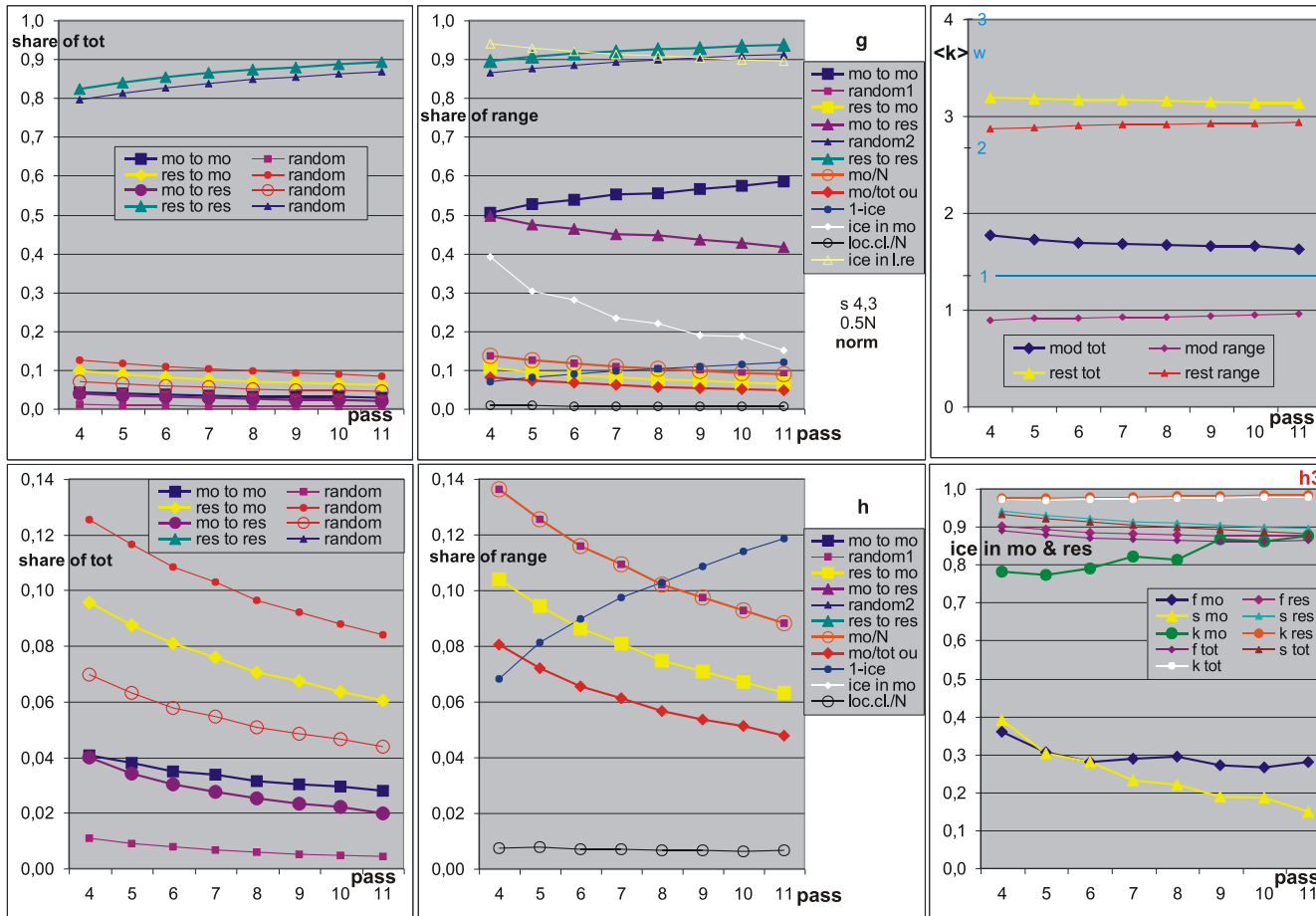


module in the network structure and, as can be seen from the charts and tables, it indicates it. Just like for individual networks in (a, b), where we could afraid that they are fluctuations, here the mo and res are more strongly connected than among themselves, and the links from mo to res are particularly rarer "to make it more difficult to get out of damage from mo to res", which is an understandable result of the selection of accumulated changes by the small change condition used in this evolution. **However, the problem remains whether it is a modification of the structure or only the selection of nodes in a random structure finding fluctuations.** The 'free' experiment and Fig.10 were supposed to answer this, but this answer only complicated the picture.

e-j – are the results from a series of 400 networks 'norm': sf (e,f), ss (g,h) and ak (i,j; k2, because s,K = 4,2) without selection specific cases, i.e. picture of the norm). Just like from the beginning, a set of nodes (which changed their state in relation to the pattern from t = 200 to tmx = 900, and the given process allowed acceptance of the change (addition of nodes to the network) that caused it) was taken as a hypothetical module.

This, however, **allows the given node in both the pattern and the studied process to be ice i.e. have a stable state, but different.** This was already observed in met5 - see ch.5.3.2. In contrast to tests a, b, c, d, individual ranges  $A1(t)$  were not determined. The lower range was set  $A1(t) > 0$ , and the upper one  $A1(t) < 5/8N$ . In preliminary studies (c, d) it turned out that the inclusion to mo nodes from processes with very small  $A1(t)$  does not significantly change the results. Since there were no selection of network cases, the average size of mo was much smaller than in (a-d), which required showing the lower parts of drawings in vertical 1 and 2 (egi) in the magnification (fhj). In contrast to (c, d), each process in a given pass of all examined networks (and not a network case) has the same weight, which was considered to be more correct.

**f3**, just like **c4**, shows what the set of mo (determined after end of pass) consists - local clusters appearing in particular processes after one initiation, similar to the clusters tested in met5 and met7, but not defined as a set of nodes with the same period of state but as nodes forming  $0 < A1(t) < 5/8N$ . These nodes were included in the mo set. As you can see, the size of such local clusters is very small here, in contrast to 'great' - selected cases in c, d. Here ('norms') the average size local cluster in the sf network only reaches about 4.5, and in ss 3.5. Of course, these are average values, because among these 400 networks there were also such as in (c, d), the average of which reached 270 for N about 530. The set mo is for 'great' in the case of sf on average 3.3 times greater than for 'norms' and ss - 5.4 times, but the local cluster is respectively 33 and 61 times greater.

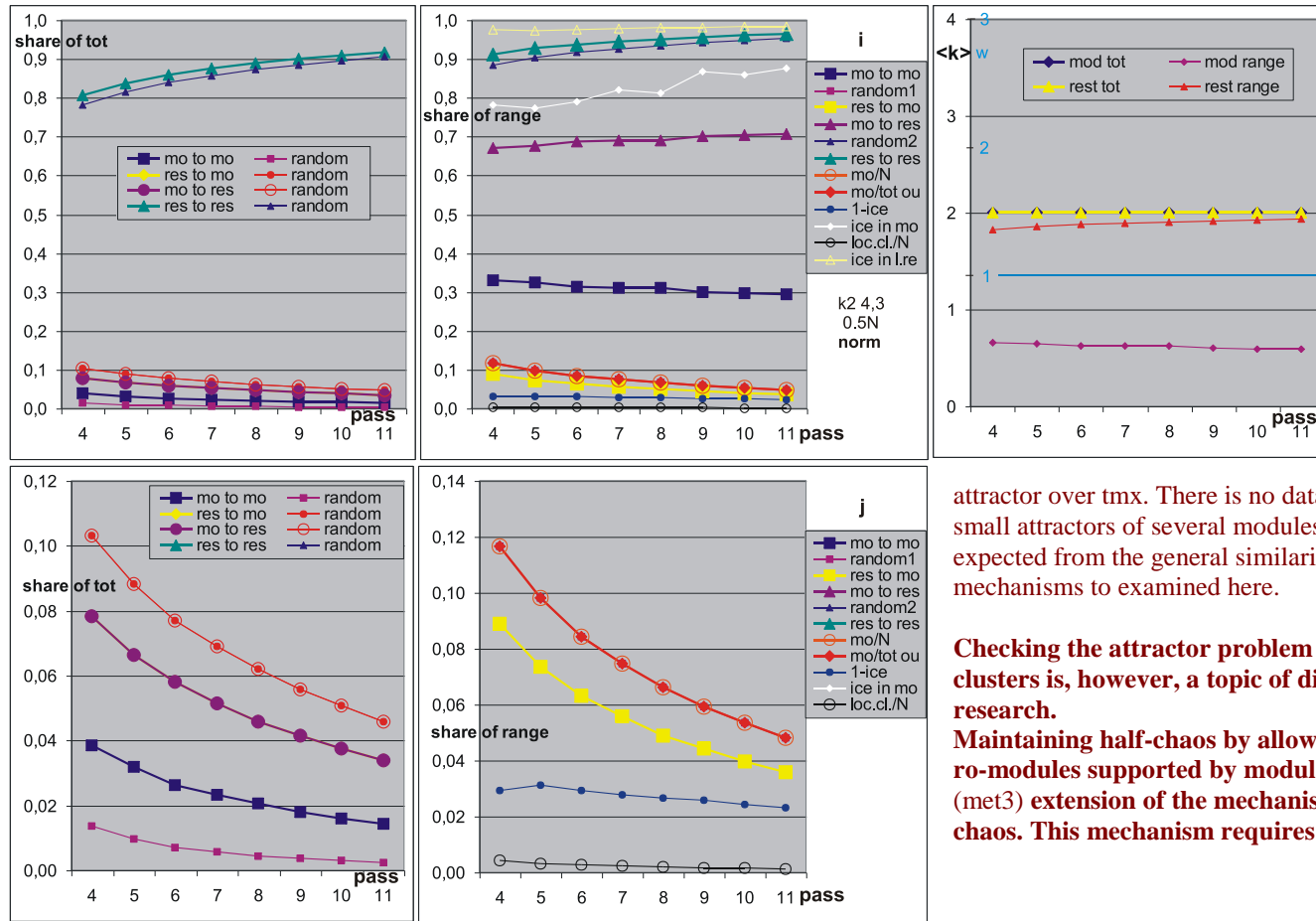


**h3** shows the share of ice in local clusters (that is also in (f3)) and in the rest of the network after subtracting of such a cluster. For comparison, the average ice at a given stage of evolution ('ice tot') is repeated, it is already shown in Fig.2  $\langle ice \rangle (M)$  and Fig.4c, and in (e2-h2). In this rest to the local clusters ('ice in res'), the ice takes about 0.9 whole, as in the whole network, but in clusters mo (ice in mo) the share of ice is significantly smaller, but it is also a significant part. This is the exact meaning of exactly the same size shown on (e2-h2) as **ice in mo**.

**In comparison with 'great', where ice in much larger clusters could practically not exist, it is a clear qualitative difference, demonstrating the difference in mechanisms.**

All three networks give a similar picture here. Mainly falls (in order of presentation: sf, ss, ak2) share of mo (0.2, 0.1, 0.07)) and mo is mo (0.67, 0.55, 0.31) in vertical 2, where also the share of mo to res increases (0.33, 0.45, 0.69; see also Fig.10).

However, the picture is clearly different from 'great'. It results mainly from a much smaller and no longer growing with evolution time, and even a decreasing mo/N, although here also the clusters mo grow ruthlessly, but slower than N.



In 'great' they grow faster due to positive feedback appearing only for larger clusters (see Fig.11), which seems to be the basic difference in their mechanism. This rapid increase in 'great' results from the permissibility of chaotic behavior in mo range within a small change (under the threshold), which makes inside mo disorders almost invisible, and this makes easier to add nodes inside. Undoubtedly, there must remain the condition of a small attractor, but here the attractor usually grows up till it ceases to be found within tmx. This further leads to frequent chaotic collapse, because the new pattern has an unchecked section of the

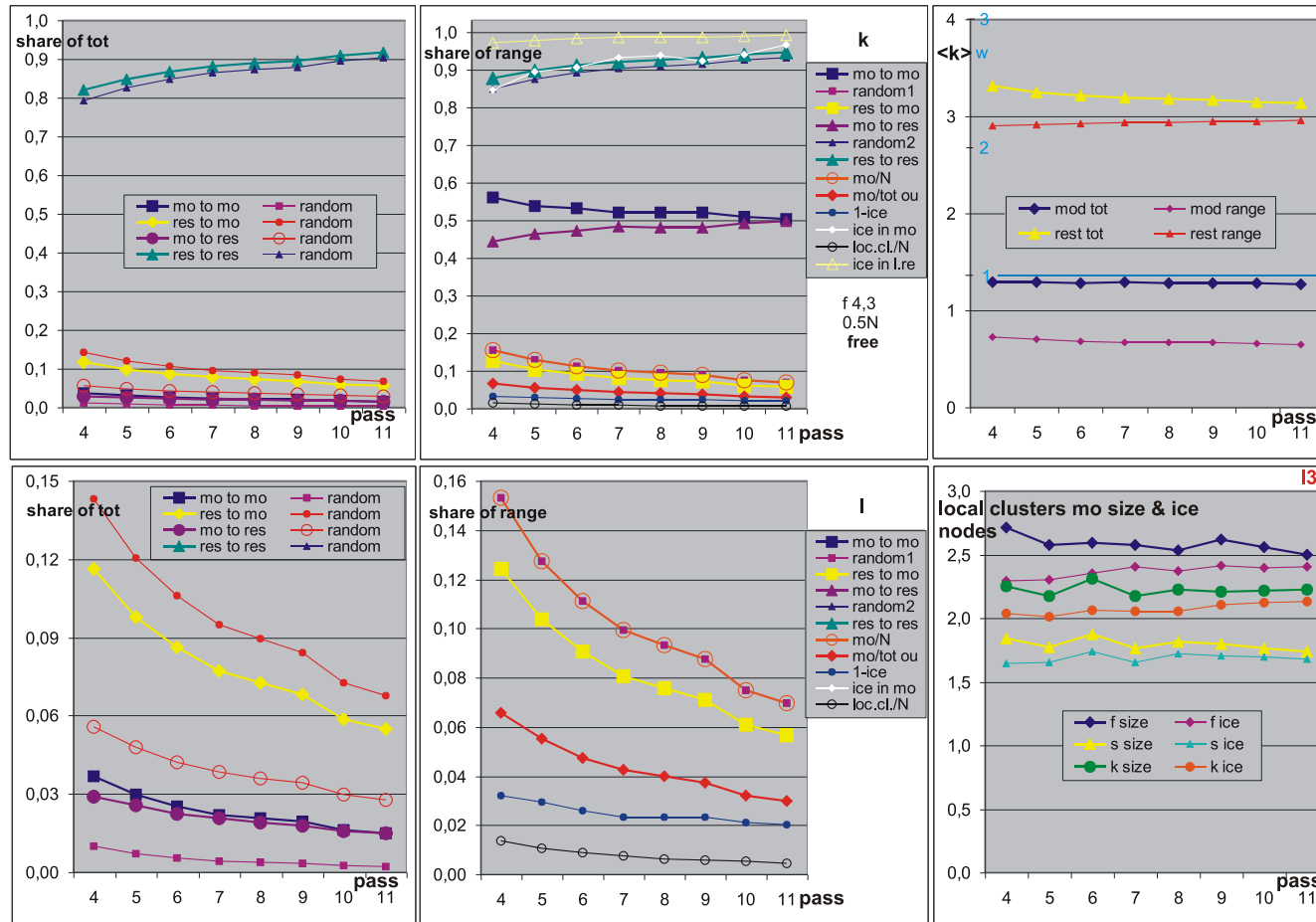
attractor over tmx. There is no data to say that attractors are assembled from small attractors of several modules that are present at the same time, but it can be expected from the general similarity of the previously studied ro-modular mechanisms to examined here.

**Checking the attractor problem and the separateness of simultaneous local clusters is, however, a topic of dispute not taken up as part of the presented research.**

**Maintaining half-chaos by allowing chaotic behavior under the threshold in ro-modules supported by modularity, is a significant but already suggested (met3) extension of the mechanisms of the evolutionary stability of half-chaos. This mechanism requires a much broader examination (see ch.8.5).**

Comparing the vertical 1, we notice that the res to res links are almost the whole in the 'norm' and their share increases, but decreases in 'great', while the remaining shares are small and are still decreasing. It is simply explained by a drop in mo/N. This is also explained by the decrease in share mo to mo in the vertical 2.

In the <k> image (egj3), a significant change is hiding of the coefficient of damage propagation inside mo under the one, which is the basis for the maintenance of the order. However, the slope is not seen, which suggests that this is only the result of choice of nodes for mo and not the evolution of the structure or correlation of functions and states. It could also be the result of evolution in the initial passes not covered by the study, but it will be shown in the 'free' study.



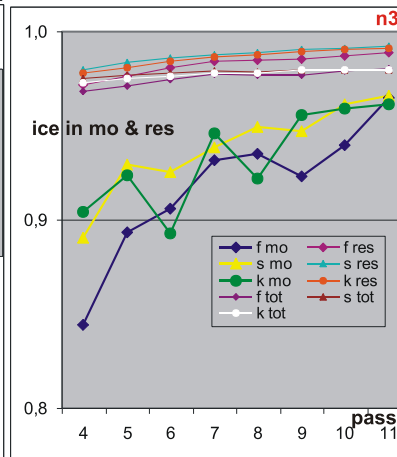
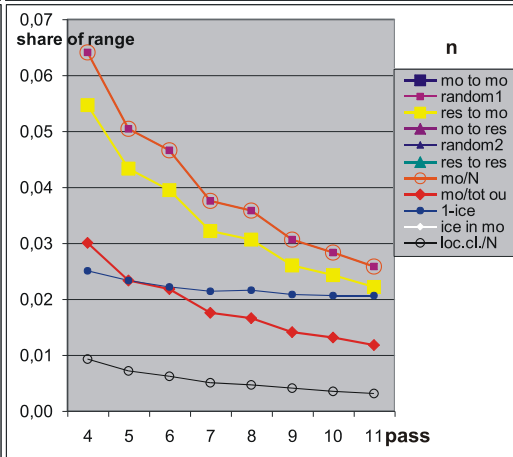
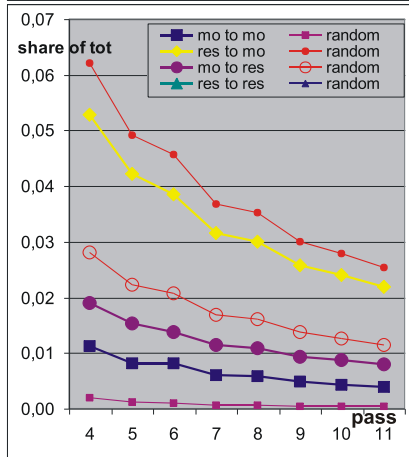
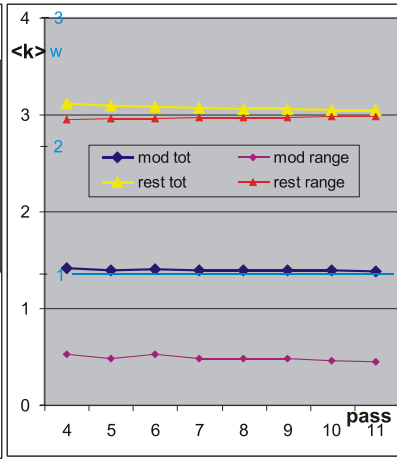
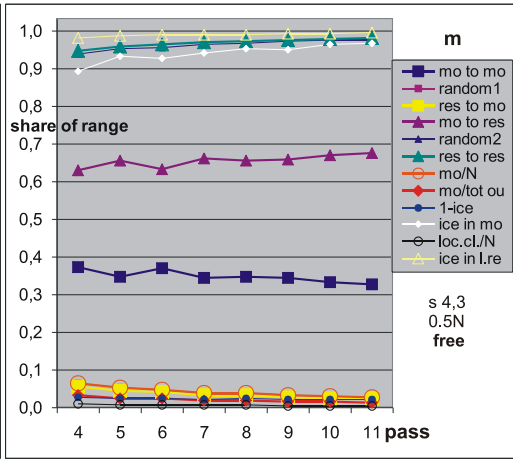
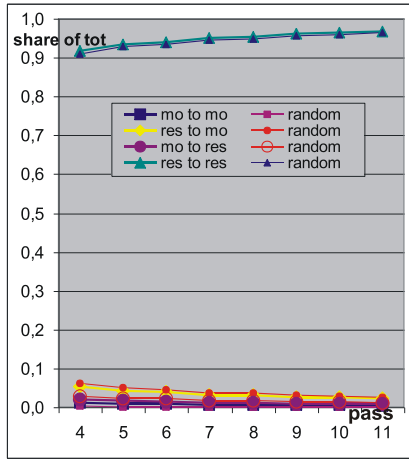
**k-p** – results of the 'free' experiment. Networks without evolution, randomly constructed as PAS, independently and in the appropriate size for each pass, not growing during this pass (i.e. no accumulation), but **'removed from the PAS'**. This 'move away from PAS' consisted in finding and accumulating a point change of function, without changing the structure, as in met1-7, with the condition of a small change, after which the pattern was no longer PAS.

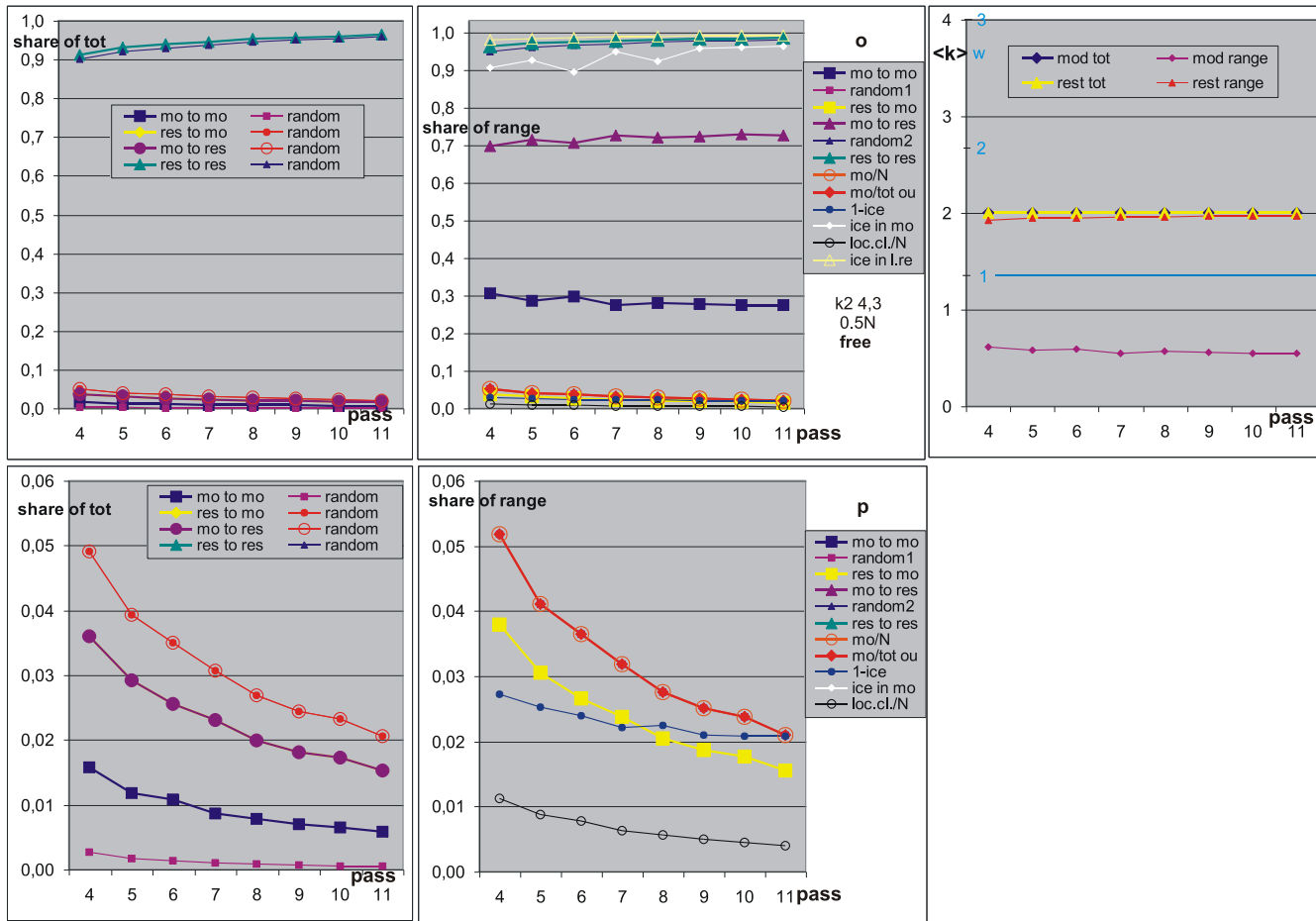
Previously, similar experience was performed without this pushing away from the PAS and it gave almost identical results, although on the crocodiles, the PAS towered as a typical accepted change, and after the withdrawal from PAS no longer.

The free experiment included 300 sets of passes 4-11 of sf, ss and ak2 networks. Because here the network is not growing during pass, the criterion for completing the pass was 100 attempts to attach the node. The image in verticals 1 and 2 is close to 'norm', it is especially similar for sf 'free' and ss networks 'norm'. This similarity results from almost identical mo/N. However, 'ice in mo' is behaving differently, which for 'norms' is relatively small and decreases, but for 'free' it is already big in pass 4 (around 0.9) and is still growing, which is better seen in (n3), whose scale starts from 0.8.

<k> also looks similar, although in 'free' also 'mod tot', i.e. the coefficient of damage propagation for all output links of nodes from mo even for the ss network is practically no longer  $w < 1$ . Here, the network ak2 (o3) breaks out, because due to its rule:  $k=K=2$ ,  $\langle k \rangle$  must be  $=2$ .

This similarity between 'free' and 'norm' is surprising. This is especially visible in Fig.10, where the deviation from randomness is calculated as in description of (a) and Fig.10. Fully random network turned out to be "the least random". This paradoxical conclusion results from the way the candidate for module is indicated - the smaller subsets are more likely to have statistical fluctuations. Unfortunately, it is not seen as clearly in Fig.9 as in Figs.10 and 12.





Here the Fig.9 ends.

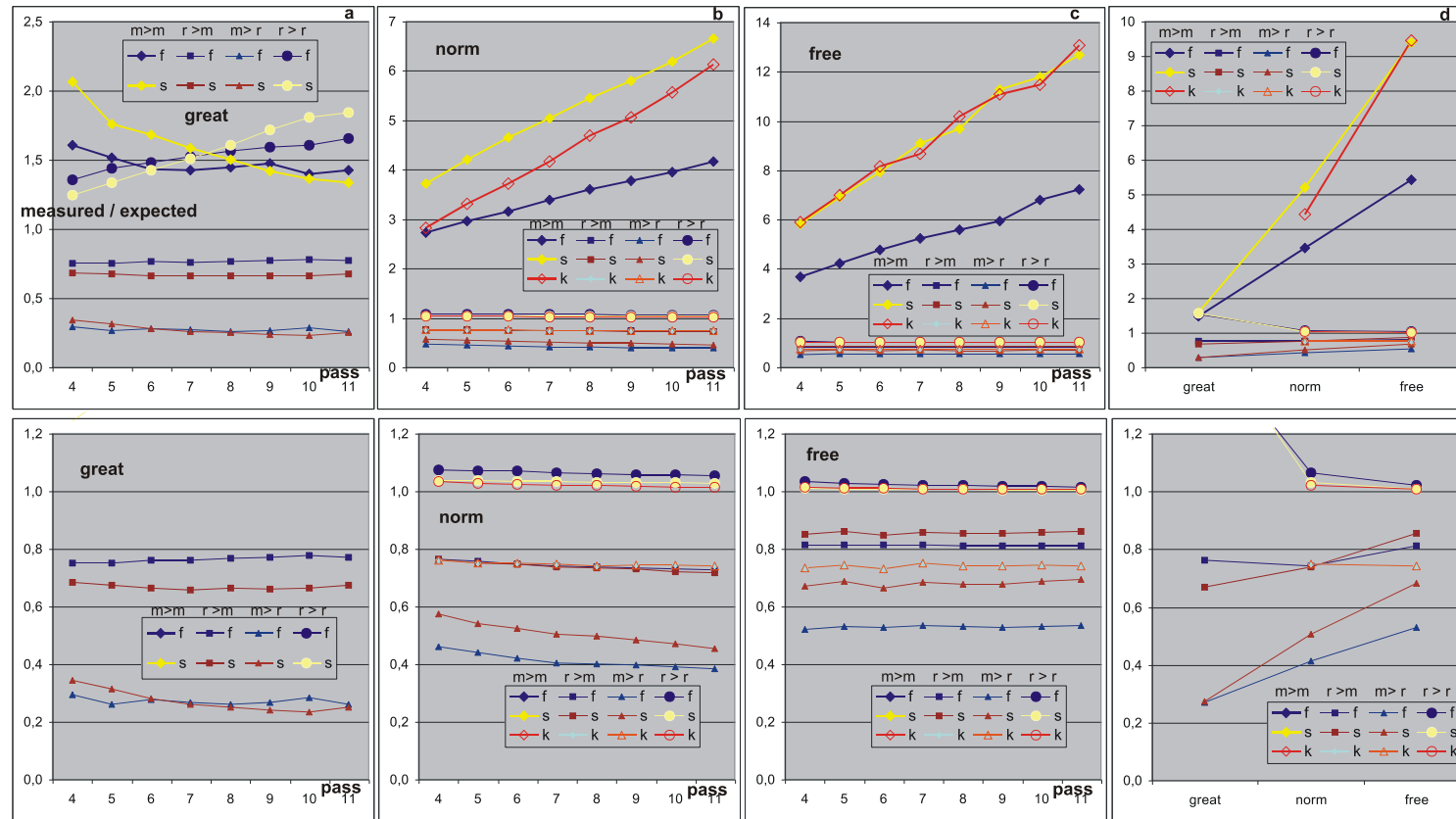


**Fig.10.** Shares of links inside and between sets mo and res compared to expectations, if there were no modular phenomena, i.e. if the links were spread evenly in the form of proportions of measured shares to expected ones. **'Great'** - selected cases based on crocodiles suspected of large modules, presented earlier in Fig.9cd; there are no cases ss 349 and ss 140 analyzed separately in Fig.9ab, although they belong to it logically. **'Norm'** - averaged results from 400 sf networks and ss networks constructed randomly in pass 1, but with evolution from pass 2 under the control of the small change condition ( $<0.5N$ ) - Fig.9.e-h. **'Free'** - Fig.9.i-l, networks without evolution, constructed in the appropriate size randomly as PAS independently for each pass and not growing during this pass (i.e. no accumulation), but **'removed from PAS'**. This 'move away from PAS' consisted in finding and accumulating point change of functions, without changing the structure, as in met1-7, with the condition of a small change. The free experiment contained 300 sets of passes 4-11 of sf and ss networks (a-c) depict the evolution of these deviations in passes 4-11, and (d) compares the mean of this evolution for the groups 'great', 'norm' and 'free'. Each of Fig. A-d has the range 0-1.2 shown enlarged underneath. The results of this statement are unexpected - the largest randomness deviation is shown by the random network! The set mo is there (over 5 for sf and 9 for ss times) stronger connected than average. This is the result of the node selection indicating the set mo on the base of participation in the acceptable process with change of state of node in comparison to pattern. It show possibility of finding such strongly connected modules in the random networks sf and ss types. It is about 2 times stronger connections than in the case of 'norm' where such selected changes were accumulated and very stronger than 'great', which suggested and exhibited real existence of modules. The explanation of this amazing result should be sought in the difference of the role of local clusters that have an inverse relationship (Fig.9c4, f3, j3) **but not further explanatory investigation has been made.** A similar experiment 'free', but without moving away from PAS gave practically exact the same results. The lack of this explanation makes impossible to resolve the question of the existence of a tendency creating modules, despite showing their presence and growth in the 'great' group. Even the current results suggest the opposite tendency - the liquidation of randomly occurring modules (although it is difficult to believe such a tendency). The problem turned out to be much more complex.

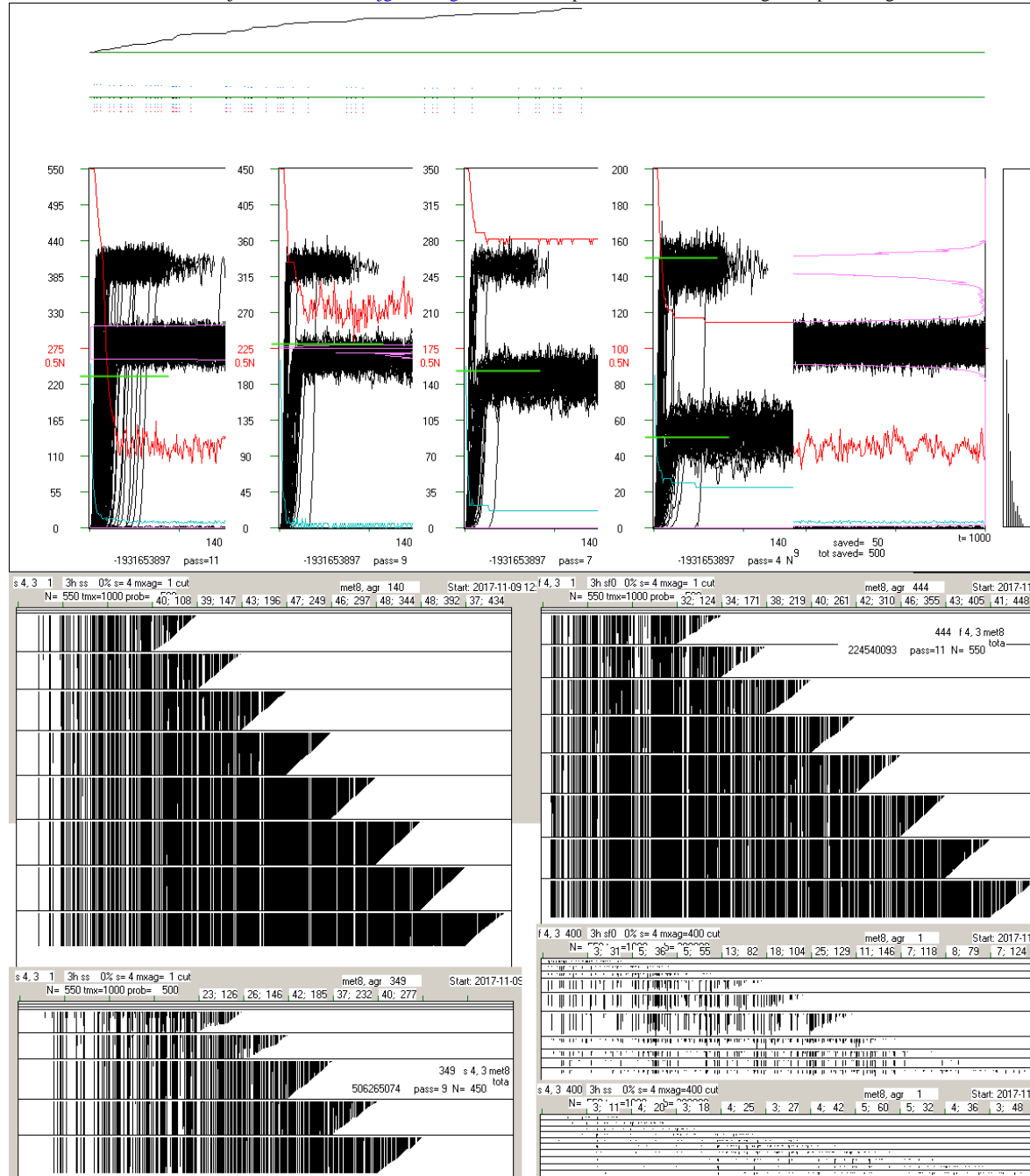


**Fig.11.** Crocodile of ss 140 as an example for the 'great' set, since ss 349 shown in Fig.6f1-4 and tested as the first in the aspect of modules (Fig.9a) had a smaller range of tested passes. For cases classified as 'great' in Figs.9 and 10., ss 349 and ss 140 are not included. Here in a fairly uniform section of the A1(t) of crocodile for pass 11 (last) the initial sections for passes 9, 7 and 4 are pasted, the end again belongs to pass 11. In these crocodiles, the expected level of Derrida balance for local clusters designated in a given pass was marked in green. The following table indicates the average size of these clusters. Assuming that Derrida chaotic equilibrium level is around  $\frac{3}{4}$  of the cluster's size, the expected levels for the clusters were determined, which are marked in green in the shown crocodile clippings.

s140 \ pass	4	5	6	7	8	9	10	11
loc.cl.size	68	95	143	210	251	309	353	306
$\frac{3}{4}$ loc.cl	51	71	108	158	188	231	265	229

Local cluster is determined only for accumulated, and here in pass 11 the large part was discarded due to  $A3 >$  threshold, which is indicated by the low level of  $q(t)$  (red line). This partly explain the miss prediction for pass 11, as the size of the cluster usually increases, and the level 265 was expected in the previous pass.

The bottom part shows the display of belonging to the set  $mo$  for nodes present in the network. **The clear downward continuity of the stripes indicates the stability of the set  $mo$**  during the evolutionary process, mainly for cases from the group 'great'. **A typical increase in the density of the bands to the right indicates the positive feedback that creates this module** and its increase. Horizontal lines separate successive passes, and at the top, 2 numbers are indicated: nodes in the local cluster (black points in the level) and processes containing  $A1(t)$  in a given range and ending with accumulation (vertical height). This image for ss 140 is located on the left under the crocodile, the others have been pasted. From the 'great' group, here is ss 349 (below ss 140, see Fig.9a and 6f1-4, although in Fig.10 and 9d it was not included to 'great') and sf 444 (right). Below two examples (sf and ss) from 'norms', here the more typical is the last - ss. Specific of 'free', in which each subsequent pass had an independently generated network, did not allow such a presentation - those passes gave an image similar to the latter one but they were, by definition, independent.

networks ('great') sf and ss were examined in the same way (there are no 'great' cases in the ak network), adding results with the same weights for each of these networks (Fig.9cd). Further similar data was collected from 400 networks of sf, ss and ak2 (K=2) without selecting cases with larger modules ('norm', Fig.9e-h). These results changed the image and interpretation of the mo and image in crocodiles - this set mo typically does not work as a module in which Derrida's chaotic balance is achieved, although such an interpretation, but with the replacement mo by a local cluster real in a single process, is correct for the special cases in the group 'great', with a large gap under the wide belt A1(t) in the crocodile with A3 under the threshold. The set mo in successive passes, compared only optically (Fig.11), was similar here (in 'great'), i.e. it had a similar composition of nodes, and the level of the observed A1(t) belt corresponded (Fig.11) to the Derrida level in local clusters whose size is only slightly smaller than mo.

Permitting chaotic behavior within the range of mo that is located under the threshold of a small change causes that disturbances inside the mo are almost insignificant, which makes it easier to add nodes inside. This is the reason for the observed positive feedback (Fig.11), where the presence of a large module affects its growth. Probably there is a condition of a small attractor, but this was not checked. The attractor usually grows significantly until it stops being found under tmx. This further leads to frequent chaotic collapse, because the new pattern has an untested section of the attractor over tmx. There is no data to show attractors assembling from several semimodules / modules present at the same time, but it can be expected from the general similarity of the mechanisms studied here to ro-modularity recognized earlier.

**Checking the attractor's problem and the separateness of simultaneous local clusters is a big topic, not taken up in the presented research.**

**Maintaining half-chaos by allowing chaotic behavior under the threshold in ro-modular assisted by modularity is an important, but already suggested (met3) extension of the mechanisms of the evolutionary stability of half-chaos. This mechanism requires a much broader examination.**

The set mo for 'norm' is often overlapping local clusters whose average size is much smaller than mo, in other words - it is a collection of nodes that give an increase in A1 in accepted processes (A3 under 0.5N threshold). Also in such a set mo, the average k is significantly smaller, and the links from mo to res are particularly rarer than estimated as random, while the links mo to mo can be significantly more frequent, although for 'great' close to res to res (Fig.10).

This image is easily understood as the result of selective pressure resulting from the condition of small change. The res set is inactive (i.e., it is not activated by damage avalanche), moreover it is mostly ice, the frequency of its links are close (especially in 'morm' and 'free') predictions based on randomness. In order for the avalanche to be small, the set may try not to release damage from itself to the rest, and minimizing damage has a smaller average node degree k, which reduces the coefficient of damage propagation w [dgc, it] (Fig.9a3-g3 except f3) associated with the Lyapunov exponent. This, however, does not have to result from the evolutionary pressure on the structure, and it can be the result of only selection when selecting nodes for the mo set.

Thus, 300 sf and ss 'free' networks were counted - without changes of structure and evolution (Figs.9k-p, 10). The results are unexpected - "the largest deviation from 'randomness' has a random network!" The set of mo is there (over 5 for sf and 9 for ss times) more strongly connected than the average. This is the result of selection of nodes for the set mo on the basis of participation (with the change of state in relation to the pattern) in acceptable processes. This shows the possibility of finding such strongly connected modules in random sf and ss or even ak2 networks. It is almost twice as strong binding than in 'norms', where changes so selected were cumulated (which should increase the effect). It is also incomparably stronger than in 'great' cases, which suggested and showed the real presence of modules. Explanations of this amazing result should be sought in the difference in the role of local clusters that have an inverse relationship (Figs.9c4, f3, j3) but no further explanatory research was undertaken.

**The lack of this explanation does not make it possible to settle the question of the existence of the tendency creating modules, despite showing their presence and growth in the 'great' group. These results even suggest the opposite tendency - the liquidation of random modules (although it is hard to believe such a tendency). The problem turned out to be much more complex, probably the observed effect consists of several different mechanisms waiting to be recognized, and correlation with the size of local clusters.**

**Summarizing: The presence of classical modules has been demonstrated in both sf, ss and ak2 networks after the evolution maintaining half-chaos as well as in random networks. This was not checked in met1-7, it had to be there, but it did not significantly affect the results. This is completed by the next chapter. 8.5.**

In the case of met8, where the structure is variable, the larger modules grow with positive feedback during evolution. It is estimated that this modularity supports ro-modularity. It was not possible to state (basing on obtained results) the tendency creating the modularity of the network as a result of the selection by a small change maintaining the half-chaos, and even the obtained results suggest an opposite tendency - blurring the separateness of modules as a result of such an evolution. However, this suggestion is too weak and the problem, which is clearly complex, requires further, much broader research, you can expect several independent mechanisms.

As you can see, the prepared basis of our concepts is not adequate for moving around in the phenomena observed in the evolution of complex networks, so for their further penetration it requires rebuilding based on the results of such research.

## 8.5 Modularity studies 'met58ro' for models c and b

This chapter shows the basics of correction - **changes of the originally used name 'semimodularity'** to a more adequate 'ro-modularity'. In subsequent works, the inference system will be matched to these bases, however, in this report, the omission of an erroneous belief that indicated the choice of an experimental path would lead to difficulties in justifying the described research. The new terminology has already replaced the old one from the beginning of this text, also in texts on viXra.

The modularity studies related to the possibility of acceptance the change initiating damage in the random networks described in the above chapter 8.4.4 showed the presence of modules in random networks, I thought that within their statistical fluctuation. In the met1-7 studies described in the first part of this report [rep] I did not take this opportunity into account, because I just did not expect it. As a result, I originally used the name 'semimodule': in the summary of the rep I wrote: 'Version of half-chaos called "semimode" based on "semimodularity" mechanism is especially interesting. Both these terms are here introduced. **Semimodularity is similar to modularity, however, it is not based on heterogeneity of connections but on specific assembling of node states and functions.**' Next, in chapter 5.1.1, I pointed out the basis of this vision: 'The third aim is to check thesis called "semimodularity", ... However, now **it cannot be the modularity based on intensity of links.**' and in the summary met5: '**Semimodularity differ to modularity fundamentally – here structure of connection is random and near even, but classic modularity is based on different density of connections.**'. This deep conviction that the random network has an even connection preventing the creation of modules is obviously a mistake, but I found the error myself. In spite of intense attempts to submit my works, their results and interpretations for discussion, direct requests to researchers dealing with this subject, no one took up the discussion, nobody carefully read the initial versions of the articles. Only the results in the met8 from the 'free' series, which gave the picture inconsistent with this belief, caused its undermining, but it did not come in first step.

Now I know that '**we can always indicate several connected nodes and this set will be more strongly connected than the average**'. The effects of modularity are always there, we cannot make a network so even that modules are not there. This trivial conclusion, which should appear at the very beginning, was noticed only after analyzing the effects in the lv network - constructed so that no node is distinguished in the network structure. Before that, however, **research returned to met5** to check the presence and correlation of modularity with the ro and A4 clusters studied there in constant random networks. These studies are the basis for the reinterpretation of met5 results, and since rep is already in the viXra archive and can only be erratum slip or small correction, these tests remain part of met8 and have been compromised with the **met58ro** name.

### 8.5.1 Sources of modules presence in random networks and their relationship to 'ro-modules'

Introduction of 'semimodules' and based on this 'semimodularity' was reasonable as using new name for observed clusters, but it was necessary to check how much **semimodularity** was supported by modularity. In the case of a strong relationship, the accuracy of the used name would be too small, while with a weak relationship - noticeable occurrence of **semimodules** without correlation with modules, such a name would be reasonable and would indicate the separate existence of such entities. Therefore, such a study was made **on the basis of the simulation program 44 '4+7' described in ch.5.7.3**, as a series **met58ro of models c and b for networks sf, er as in met5 and** additionally for the **ss network**. There 40 networks that came to M20 was simulated, treating it initially as a diagnosis, but it was enough. (Increasing the number of cases would require significant modifications of the program.) Because in M20 the attractor can not decrease, which increases the number of local ro clusters occurring in it without increasing the number of global clusters (**m5.Fig.19b**), the state was examined after M19 - simpler in this respect and the most stable.

**Four different ways of selecting the set 'mo' - candidate for the module were examined.** First and foremost, the same rule was used, which in such a surprising result caused a return to met5. Unfortunately, it gave a set of mo containing almost the entire network, which in met5 has  $N = 400$ . In the network cf (model c, sf network) on average 6.5 nodes remained outside the mo set, and in the remaining 5 cases at least a row less, which completely deprived sense of further analysis.

The second most important candidates were global clusters ro. As can be seen from **m5.Fig.19b**, there are on average just over 2 of them, so 2 - ro1 and ro2 were examined in **Fig.12**. The relatively frequent lack of ro2 (around 12 per 40) did not change much in accuracy. The average share in the network so designated mo is presented in **Fig.12ad and the table in this figure**. These are small sets, so random statistical fluctuations in the random network may give larger deviations here. As can be seen in **Fig.12be**, the deviation from the predictions for 'mo to mo' links reaches 102 times (ro2 cr), least 20 times (ro1 cf), and in model b this range is 11 (ro1 bs) to almost 29 (ro2 br), see **table in description Fig.12**. It follows that ro clusters as **semimodules are also usually modules, despite the random network**. The method of indicating the mo in met8 for the random network gave this deviation only about 9.5 times for ss and ak2, and for sf about 5.5 (**Fig.12d**). **Semimodules** in the form of global ro clusters in met5 investigations indicate modules in the random network much more efficiently, however, their size is usually much smaller than the mo sets in met8.

The third candidates are the A4 clusters (ch.4.6.3 and 5.6.4, as well as 6.4.2, 7.4.6, 7.5.6). Two clusters A41 and A42 were also studied here, but the largest ones were selected. It turned out that, similar to the method used in met8, A41 was usually too large (Fig.12ad) and gave a too specific image in Fig.12bcef, so that it would be reliable for A4 clusters. On the other hand, A42 gave an image similar to ro1 and ro2, although clearly more radical (see table).

The last candidate was the sum of all A4 clusters, which was very little different from the mo used in met8.

So the question arose: **does modularity replace semimodularity in met5 and met7 research?** And further: **Is it possible to build a network that is sufficiently random to receive half-chaos, starting from PAS, but without modularity?** Such a network would allow to save endangered 'semimodules'. An attempt was made to construct it, assuming that every node in the structure of this network should have the same properties. I have already used networks extremely simple in [it] for explanation, they were networks based on the 'aggregate of automata' ( $K = k$ ), used in the met8 network ak with  $K=k=2$  is such a network. Also the lv network is a special case of it: first input link of given node (a) gets a signal from the node (d) of the number 20 more ( $d=a+20$ ), and the second from the node  $d=a+19*(a \bmod 19 + 1)$ , where it always final  $d:=d \bmod 399$ . A met58ro simulation was also performed for such a network, and its results are also shown in Figs.12, 13, 14.

**Even in such the network lv modules appeared, although it is not random and there is no fluctuation in it.** Then it turned out that we can always indicate a few connected nodes and such a set will be more strongly related than the average, so modules are always, you can not make a network (with a sensible K) so even that modules would not exist inside. At the same time, it turned out in a meticulous analysis of the obtained results that each global cluster was built of nodes more closely related to each other, which was clear from the beginning, but that is why they form a formal module. In this way, **the basics of the name 'semimodules' turned out to be wrong**, the ro clusters detected in met5 are simultaneously modules and **the prefix 'semi' is unjustified**.

In met7 'semimodules' were built (now -ro-modules) as if without correlation with modules, but many of them turned out to be ineffective, and in many as a semimodule, in effect acted part of such a construction. When they were constructed, connections were made, so that in one 'semimodule' there were nodes connected with each other and not with other 'semimodules'. It was assumed that the density of connections is even, 'because it results from the randomness of the network structure'. These assumptions, however, did not provide, because they could not, the lack of modules, and even as a result, constructed 'semimodules' became modules.

**After this significant correction of the interpretation, the basic conclusions and experimental facts remain unchanged: half-chaos exists, has evolutionary stability even with such significant initiating changes as adding and removing nodes, occurs even in such a non-random network as lv.** The correction concerns only the name 'semimodule' and the resulting name of 'semimodularity' and the suggested beliefs underlying the adoption of such a name based on the belief that random networks do not contain modules, so the observed clusters can not be them. While ro clusters in replacement of semimodules may suffice, **semimodularity** as the name of the whole mechanism in which ice occurs, and in it isolated, active areas, should be replaced by a new name: ro-modularity. With this choice, **we can replace the semimodule with a ro-module**. On this basis, corrections were made to the texts of rep and Naaj on viXra and in this text here from the beginning.

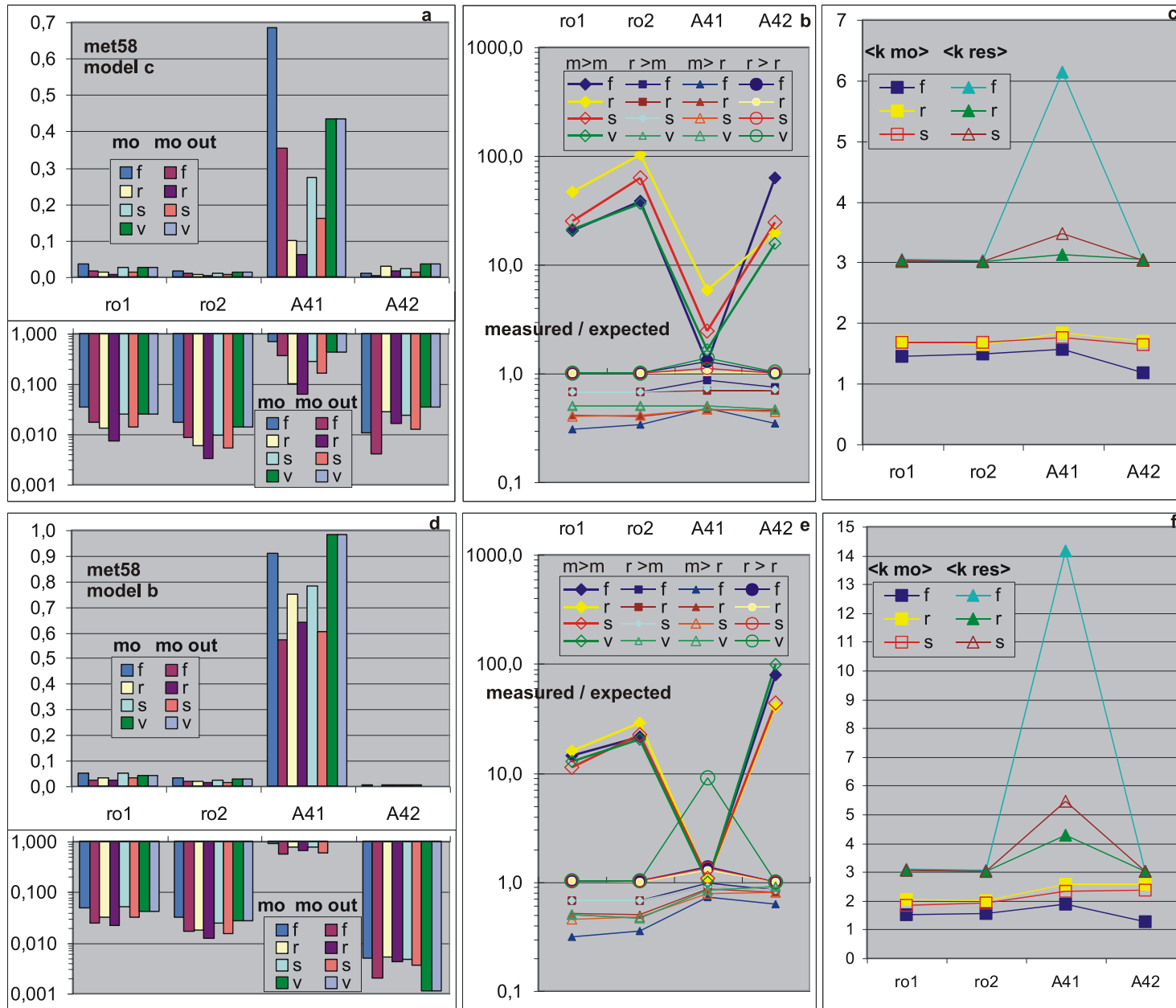
		sf			er			ss			lv		
		ro1	ro2	A42	ro1	ro2	A42	ro1	ro2	A42	ro1	ro2	A42
met58c	mo	0,034	0,017	0,010	0,012	0,006	0,028	0,025	0,010	0,023	0,024	0,014	0,035
	m>m	20,47	38,29	62,74	45,89	102,30	19,74	24,77	61,90	24,26	20,94	36,11	15,71
	r>m	0,67	0,67	0,75	0,67	0,67	0,69	0,67	0,67	0,70	0,50	0,50	0,47
	m>r	0,30	0,34	0,35	0,41	0,40	0,45	0,40	0,41	0,45	0,50	0,50	0,47
	r>r	1,01	1,01	1,00	1,00	1,00	1,01	1,01	1,00	1,01	1,01	1,01	1,02
met58b	mo	0,049	0,031	0,005	0,032	0,018	0,005	0,051	0,024	0,005	0,042	0,027	0,001
	m>m	14,22	21,00	79,54	15,77	28,72	40,27	11,15	22,47	43,74	12,58	20,27	98,52
	r>m	0,67	0,67	0,84	0,67	0,67	0,83	0,67	0,67	0,85	0,50	0,46	0,89
	m>r	0,32	0,35	0,62	0,51	0,49	0,80	0,45	0,48	0,80	0,50	0,46	0,89
	r>r	1,02	1,01	1,00	1,01	1,01	1,00	1,02	1,01	1,00	1,02	1,01	1,00

**Fig.12. Search results for modules in the series met58 ro '4+7'.**

Within this figure there is a table showing, in numerical form, the more important results shown in drawings - the share of the so-designated set mo (a,d) and deviation from random predictions in the form measurement / expectations (b,e).

The results of simulations of sf, er networks were presented here, which were tested in met5 from the beginning, but not in the aspect of modularity, and ss network used in met8 instead of er, and additionally lv networks with quite non-random and possibly even connections, which were to eliminate fluctuations originally suspected of creating modularity. It is now known that modules

are present always and do not require fluctuations, but this network remains a good basis for creating the correct intuition of half-chaos mechanisms, which is similarly strong in other networks (Figs.13, 14). So it is a valuable complement to met5.



The figure contains 2 lines, the upper one of which concerns model c - the basic for conclusions from met5, and the lower - model b with minimal regulation (see met4).

(ad) shows the shares of the mo in network and the output links from mo among all exit output links. These 2 factors define the predictions for (be) and in the table. For lv  $K=k=2$  for each node, both factors are the same. For A41 mo is particularly large, which has a clear reflection in (bcf) indicating the uniqueness of this cluster.

Due to the large span of the presented values, the log scale at the bottom and the more easily readable line scale at the top were used here.

(be) on the log scale represents a deviation from expectations, which is significantly stronger here than in met8 in Fig.10. See also the table. The sets mo are significantly stronger connected here than res, which coincides with the expectation, but the links between them are less frequent than expected, so they are modules. A41 has a different character.

(cf) represents the mean number of output links for mo and res. Excluding A41, res has the expected value of 3 resulting from  $K=3$ , and mo, like in met8,

has clearly lower values, which reduces the coefficient of damage propagation (see vertical 3 in Fig.9). For lv  $K=k=2$  are constant, so here lv is not shown.

### 8.5.2 Simulation results for ss and lv networks complementing met5 results

The ss and lv networks are qualitatively different from the sf and er networks, which were the basis for conclusions from met5. Since the evolution of these networks has already been simulated in the met5 research formula, it would be strange if their results were not compared to earlier ones. Generally, these are very similar results, although the differences are not significant for the main conclusions. First of all, the non-random network lv with  $K=k=2$  gives the right peak on the damage size distribution clearly shifted to the left (which results from  $K=2$  and is also visible for ak2 in Fig.1), more strongly for the formula b containing regulation. This is presented in Fig.13. As usual, the diagram dividing initiations into ordered (in the left peak) and chaotic (in the right peak) is included. It clearly indicates that starting from PAS we get a half-chaos even in a non-random (in structure) network like lv, which also confirms pasted  $P(akc|M)$ . The shape of the left peak is also similar to other studies in met5 and met7, but different from met6, where also the modules must be, but there is no ice and ro-modularity.

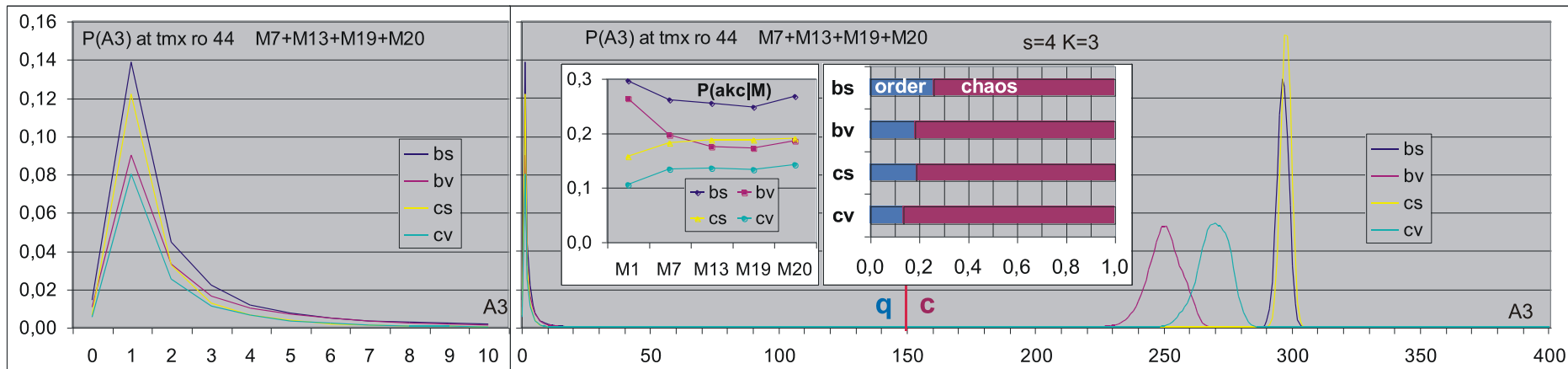


**Fig.13. The basic result for the ss and lv network in met58, complementing the met5 study (m5.Fig.20 for sf and er networks).** Two peaks in the distribution of damage size in the form of  $P(A3)$  (compare to Fig.1). The left peak shown more precisely has a shape similar to the other networks in met5 and met7, even for a particularly non-random one in terms of connections between the nodes of the lv network. This shape is also different from the one received in met6. The right peak for lv is clear, but also clearly shifted to the left and wider, which results from  $K=2$  and is also visible for ak2 in Fig.1. The gap between the left and right peaks is clear. The pasted diagram of the degree of order  $q$  and chaos  $c$  even shows the presence of order for lv, and the graph  $P(akc|M)$  for the Mfree passes shows stability  $q$  in evolution. Together, it shows a similar half-chaos as in previous met5 studies for sf and er networks.

Complementing the met5 simulations of the next networks: ss and lv, above all should be referred to the differences with m5.Fig.19 showing 'statistics of local and global clusters which create ro-modularity'. In the area 'm5.Fig.19a - Distributions of size of local clusters and ice for formulas bf,br,cf,cr in dependency on M - passes free describing level of advancement of shift from PAS0.' does not make sense to present the distributions for ss and lv, as they are sufficiently similar: bs and bv to bf, and cs and cv to cr. The basic differences here are roughly Fig.14f 'range' - the range of sizes of local clusters and ice. This is the first point where the sum of tail counts exceeds the value of 2 (for comparison with m5.Fig.19a, because now there are 40 networks and that there were 100, although now it is slightly too small statistic). For clusters, this is a range from 0 to the height of the post, and for ice from the top end of the post to 400.

Analogous charts as in m5.Fig.19b are presented for ss and lv networks in Fig.14a-d. Here the similarities are also strong, but it is difficult to indicate such simple rules as above, although you can also see the differences, but it is worth looking when the needs occur. On the other hand, m5.Fig.19c differs systematically in a similar way for all four formulas, and this issue has not been analyzed now, an example indicating the direction and nature of this difference is in Fig.14e. The less important data analogous to m5.Fig.19de was omitted.

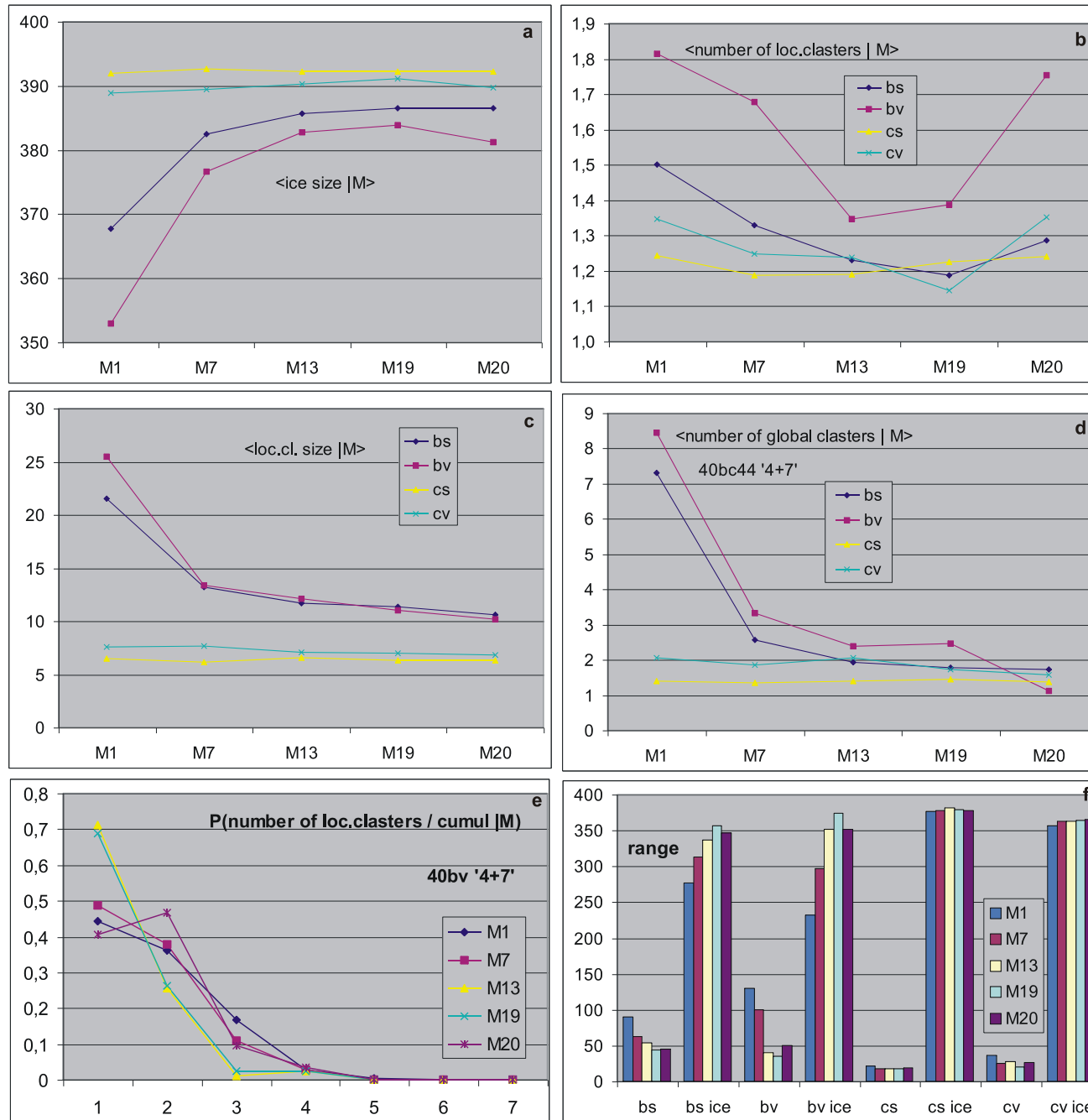


**Fig.14. More important statistics of the local and global clusters for creating ro-modularity, obtained in the met58ro simulation for ss and lv networks, which differ from obtained for the sf and er networks presented in m5.Fig.19.**

In the scope of 'm5.Fig.19a - Distributions of size of local clusters and ice for formulas bf,br,cf,cr in dependency on M - passes free describing level of advancement of shift from PAS0', the basic small differences here show roughly (f) - the range of local clusters and ice sizes. This is the first point in which the sum of tail counts exceeds the value 2. This is a bit too small statistic, but sufficient for comparison with m5.Fig.19a, where the more sensible value of 5 but for 100 networks was used. There are 40 networks here. For clusters, this is a range from 0 to the height of the post, and for ice from the top end of the post to 400.

(a-d) - Average sizes of ice (a), local clusters (c) and average number of local (b) and global clusters (d) for bs, bv, cs, cv in dependency on M - free passes depicting how far away is from PAS0. Since there are several local clusters, the sum of the average ice and average size of clusters does not give 400. As in m5.Fig.19b, a particularly large number of global clusters for the pass M1 in the model b is striking. For the ss and lv networks the minimum in (b) is around 1.3 when for sf and er it was around 1.8.

(e) - Distributions of the number of local clusters depending on M presented in m5.Fig.19c were clearly different from each other, here they are more similar to each other, but different than that. Here, M13 and M19 are very similar, but slightly different from M1, M7 and M20, which are similar.

## 8.6 Summary

Investigations met8 has shown that damage initiations in the form of adding or removing of nodes, although they are rather large disturbances in comparison to the permanent point change of function used in met1-7, also give half-chaos when the start from the point attractor. The mechanism of this half-chaos is also based on the maintenance of a large fraction of ice, which strongly suggest ro-modularity. However, clusters ro were not controlled here, so the ro-modularity has not been thoroughly checked.

The presence of classic modules has been demonstrated in sf, ss and ak2 networks (ak with  $K=k=2$ ) after the evolution maintaining the half-chaos as well as in random networks, i.e. the presence of modularity has been demonstrated. In the case of met8, where the structure is variable, the larger modules grow with positive feedback during evolution.

In previous met1-7 studies on the random network of constant structure [rep], the presence of modules was not expected and not checked, but the results of the current met8 indicate that they also had to occur there. This has a significant impact on the interpretation, so we returned to met5 research in the series met58ro, where the presence of modules strictly correlating with the ro-modules was found. As a result, the term 'semimodule' was removed and replaced with 'ro-module', and the mechanism based on the presence of small, independent 'lakes' in the ice was called 'ro-modularity' (previously: 'semimodularity').

It has not been found a base to state the tendency creating the modularity of the network as a result of the selection with a small change maintaining the half-chaos, and even the obtained results suggest an opposite tendency - blurring the separateness of modules as a result of such an evolution. However, this suggestion is too weak and the problem, which is clearly complex, requires further, much broader research.

However, a tendency of greater conservativeness of older nodes was found. It was shown that this component of the phenomenon does not result from the increase in the node degree (the number  $k$  of the outputs from the nodes) in the sf and ss networks, but is added to such an effect. This is one of the simplest elements of regularity formulated in 1940 by de Beer as terminal variability and conservativeness of the early stages of ontogenesis.